AD-A219 369

AFGL-TR-89-0080
ENVIRONMENTAL RESEARCH PAPERS, NO. 1025

Temporal Attributes of the Ambient Seismo-Acoustic Environment: La Junta, Colorado

JAMES C. BATTIS
CHRISTOPHER J. CENTER

13 March 1989

EARTH SCIENCES DIVISION
PROJECT 7600
AIR FORCE GEOPHYSICS LABORATORY
HANSCOM AFB, MA 01731

UNCLASSIFIED
SECURITY CLASSIFICATION OF THIS PAGE

REPORT DOCUMENTATION PAGE

1a REPORT SECURITY CLASSIFICATION UNCLASSIFIED	1b RESTRICTIVE MARKINGS
2a SECURITY CLASSIFICATION AUTHORITY	3 DISTRIBUTION / AVAILABILITY OF REPORT Approved for Public Release: Distribution Unlimited
2b. DECLASSIFICATION / DOWNGRADING SCHEDULE	
4. PERFORMING ORGANIZATION REPORT NUMBER(S) AFGL-TR-89-0080 ERP NO. 1025	5. MONITORING ORGANIZATION REPORT NUMBER(S)
6a. NAME OF PERFORMING ORGANIZATION Air Force Geophysics Laboratory 6b. OFFICE SYMBOL (If applicable) LWH	7a. NAME OF MONITORING ORGANIZATION
6c. ADDRESS (City, State, and ZIP Code) Hanscom Air Force Base Massachusetts 01731-5000	7b. ADDRESS (City, State, and ZIP Code)
8a. NAME OF FUNDING / SPONSORING ORGANIZATION 8b. OFFICE SYMBOL (If applicable)	9. PROCUREMENT INSTRUMENT IDENTIFICATION NUMBER
8c. ADDRESS (City, State, and ZIP Code)	10. SOURCE OF FUNDING NUMBERS PROGRAM ELEMENT NO. 621010F; PROJECT NO. 7600; TASK NO. 09; WORK UNIT ACCESSION NO. 07

11. TITLE (Include Security Classification)
TEMPORAL ATTRIBUTES OF THE AMBIENT SEISMO-ACOUSTIC ENVIRONMENT: LA JUNTA, COLORADO

12. PERSONAL AUTHOR(S)
James C. Battis and Christopher J. Center*

13a. TYPE OF REPORT	13b. TIME COVERED	14. DATE OF REPORT (Year, Month, Day)	15. PAGE COUNT
Scientific, Interim	FROM 1 Oct 86 TO 1 Oct 88	1989 March 13	48

16. SUPPLEMENTARY NOTATION
*Weston Observatory
Boston College ~ Weston, MA

17. COSATI CODES			18. SUBJECT TERMS (Continue on reverse if necessary and identify by block number)
FIELD	GROUP	SUB-GROUP	
			SEISMIC NOISE; SEISMO-ACOUSTICS; PRESSURE NOISE; LA JUNTA

19. ABSTRACT (Continue on reverse if necessary and identify by block number)

During the period 9 to 29 October 1986, seismic and atmospheric pressure data were recorded at the AFGL operated array at La Junta, Colorado. The purpose of this effort was to develop statistical models of the noise environments at this site for use in defining event detection capabilities of the array. Analysis of these data demonstrates that peak noise amplitudes for 1-second windows could adequately be modeled as Type II Gumbel extreme value distributions, EX_{II} (u,K). Further, it was shown that there is at best only weak correlation between the noise fields in both a broad-and narrow-band sense.

20. DISTRIBUTION / AVAILABILITY OF ABSTRACT ☐ UNCLASSIFIED/UNLIMITED ☒ SAME AS RPT ☐ DTIC USERS	21. ABSTRACT SECURITY CLASSIFICATION UNCLASSIFIED
22a. NAME OF RESPONSIBLE INDIVIDUAL JAMES C. BATTIS	22b. TELEPHONE (Include Area Code) (617) 377-3078 22c. OFFICE SYMBOL LWH

DD FORM 1473, 84 MAR 83 APR edition may be used until exhausted
All other editions are obsolete.

SECURITY CLASSIFICATION OF THIS PAGE

Contents

Illustrations

Tables

GLOSSARY OF ABBREVIATIONS, UNITS AND NOMENCLATURE

AFGL - Air Force Geophysics Laboratory

GDAS - Geophysical Data Acquisition System

km - kilometers (0.54 nautical miles)

Pa - Pascal or 1 newton/meter^2 (0.000145 pounds/inch^2)

PSD - Power spectral density

RMS - Root mean squared

SAC - Strategic Air Command

SD - Standard deviation

SDAS - Stand Alone Data Acquisition System

$C_{ij}(f)$ - Coherency function between channels i and j

d_{ij} - Kronecker delta ($d_{ii} = 1$: $d_{ij} = 0$ for $i = j$)

f^N - Nyquist frequency

f^S - Sampling frequency (samples/sec)

$G_{ij}(f)$ - Cross-spectral density function between channels i and j

$G_{ii}(f)$ - Auto-spectral density function for channel i

$G^s_{ij}(f)$ - Signal spectral density function based on coherent spectrum between collocated channels i and j

$G^n_{ij}z(f)$ - Additive system noise spectrum based on the incoherent spectrum between collocated channels i and j

$p_i(f)$ - Protection ratio for channel i

S/N - Signal to noise ratio for additive noise only

S/N' - Signal to noise ratio for aliased and additive noise

$T_i(f)$ - System transfer function for channel i

Temporal Attributes of the Ambient Seismo-Acoustic Environment: LaJunta, Colorado

1. INTRODUCTION

In June 1986, the Air Force Geophysics Laboratory established a semi-permanent seismo-acoustic monitoring array near La Junta, Colorado. This site, located under a SAC low-level training route, was used to investigate the potential value of seismo-acoustic techniques to detect and track low-flying aircraft. As a foundation for this work it was necessary to establish a base measure of the seismic and atmospheric pressure background levels at the site and to define any quantitative relationship between the seismic and pressure noise. The results provided in this report are based on the environment as measured during the period 9 through 29 October 1986.

2. RESULTS

It is the purpose of this paper to establish the attributes of the base seismic and atmospheric pressure noise for a surface array at La Junta, Colorado, for periods free of conspicuous events. Further, it was desired to establish the level of correlation between

Received for Publication 3 March 1989

surface pressure and seismic noise at this site. Due to the nature of seismo-acoustic coupling, the main interest is in the relationships between vertical seismic noise and atmospheric pressure. General statements of the findings of this study can be given as:

(1) The seismic and pressure noise levels observed at the La Junta site in the band 1 to 30 Hz are significantly above measurement system noise;

(2) The seismic and pressure noise environments are neither Gaussian nor stationary and show distinct temporal variations probably associated with meteorological conditions;

(3) The maximum envelope levels for noise at this site, taken over 1.01-sec windows, can be adequately represented for the purposes of detection threshold estimation by Gumbel Type II extreme-value distributions, $EX_{II}(u,K)$. The parameters of these distributions are [$u = 3.8 \times 10^{-5}$, $K = 2.56$] and [$u = 9.1 \times 10^{-5}$, $K = 2.29$] for vertical and horizontal seismics, respectively, and [$u = 0.108$, $k = 2.12$] for the atmospheric pressure field; and, finally,

(4) The seismic noise environment at the La Junta site is only weakly correlated with the total atmospheric pressure signal in the same band, and the vertical and horizontal seismic noise conditions are also only weakly correlated.

3. SITE DESCRIPTION

3.1 General Description

La Junta, Colorado is located along the Arkansas River valley in southeastern Colorado and is approximately 100 kilometers east-southeast of Pueblo, Colorado (Figure 1). The site is typical of the high plains of eastern Colorado with relatively shallow relief and semi-arid vegetation consisting of sparse grasses and sage brush. The property surrounding the site is used as cattle range land.

3.2 Cultural Setting

The towns of La Junta and Los Animas lie about 20 km to the west and 22 km to the northeast of the site (Figure 2). A multi-lane highway trends east-west about 13 km north of the site and runs along the course of the Arkansas River. The highway is paralleled by an active main line of the Santa Fe Railroad. A ranch service road runs approximately 200 m south of the site and the ranch manager's home is located about 1.5 km to the southeast.

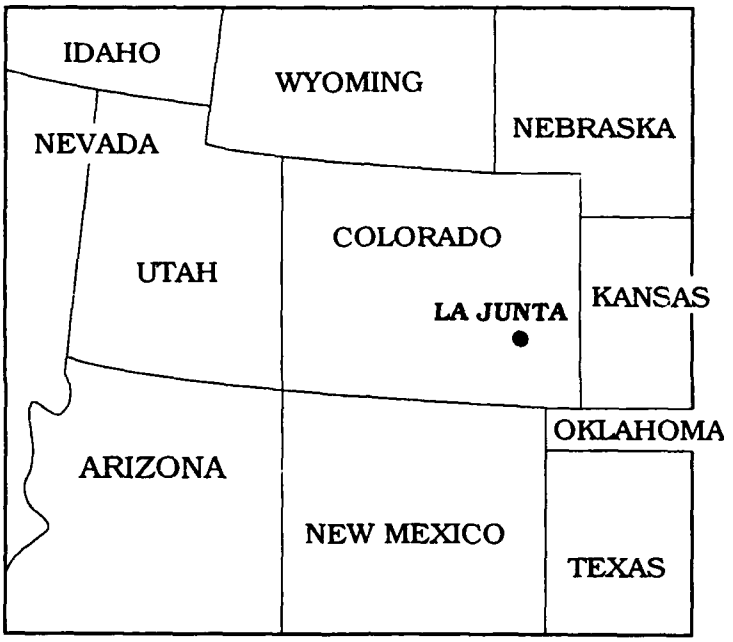

Figure 1. Map Showing the General Location of the AFGL La Junta, Colorado Seismo-acoustic Monitoring Array.

Of particular interest for the vibro-acoustic environment of the site is the fact that the array lies under a SAC low-level training route used by B-1, B-52, and F-111 bomber aircraft. In this route SAC aircraft are permitted to fly as low as 130 meters. The La Junta site is essentially in the middle of the 16.5 km-wide training route corridor. However, typical aircraft flight paths take them within approximately 1 km east or west of the site.

3.3 Geologic Setting

The site is located 1300 m above sea level on a flat plain running out to the east from a SSW trending ridge line about 100 m above the surrounding terrain. The surface layers appear to be fine grained, sandy soils with a shallow caliche layer. It can be assumed that these layers are largely the deposits from the erosion of the ridge line to the west of the site.

Physiographically, the site lies on the western margin of the stable continental interior of North America.[1] Although the deeper structure has not been studied for this report, it can be assumed that it is typical of the region, consisting of largely undisturbed sedimentary rocks laid down under the Cretaceous epicontinental sea. Since the Devonian, the dominant

[1] Clark, T., and Stearn, C. (1960) *The Geological Evolution of North America*, The Ronald Press Co., New York.

tectonic process for the region has been a general uplift associated with the episodic orgenies of the Rocky Mountains.

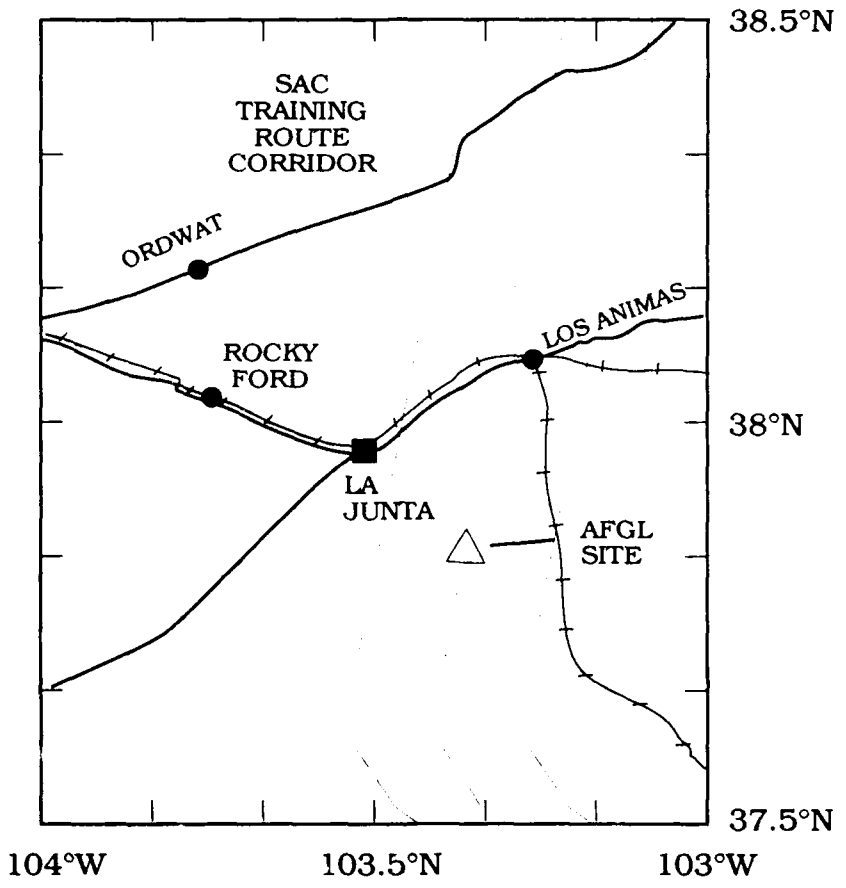

Figure 2. Map Showing the AFGL Seismo-acoustic Array, Local Topography, and Major Cultural Noise Sources in the Area.

4. GEOPHYSICAL DATA ACQUISITION SYSTEM

4.1 General Description

The seismo-acoustic measurement system used at the La Junta site was an upgraded Standalone Data Acquisition System (SDAS) as described by von Glahn.[2] This package, the

[2] von Glahn, P.G. (1980) *The Air Force Geophysics Laboratory Standalone Data Acquisition System: A Functional Description*, AFGL Report No. AFGL-TR-80-0317, ADA160253.

Geophysical Data Acquisition System (GDAS), is a unified multi-channel data sampling, signal conditioning, and processing system. Data used in this report were acquired with the GDAS recording four seismometers, two vertical and two orthogonal horizontal instruments, and three pressure transducers. All of the sensors were collocated for estimation of system generated noise. (Collocated, as used here, is defined to mean that the distances between sensors is less than 0.1 times the shortest wavelength anticipated within the system pass band.)

The seismic environment was measured using Hall-Sears HS-10-1B velocity transducers. These instruments are characterized by nominal natural frequencies of 1 Hz and intrinsic sensitivities of the order of 1200 volts/(meter/sec). Pressure sensors used were DJ Instruments MLR +/- 3450 Pascal differential transducers. A low pass anti-aliasing filter, having a corner frequency of 35 Hz and a roll-off of 36 dB/octive, was applied to the data. This provided nominally flat system responses between 1 and 30 Hz for both seismic and pressure signals.

During data collection, the GDAS was programmed to record 30-sec noise samples at 5-hour intervals for all available channels. A sampling rate of 100 samples/sec was used for all channels and sample sequences.

4.2 Channel Response Calibrations

The seismic channels were calibrated *in-situ* by application of a known current to the calibration coils of the seismometers. This is equivalent to the application of a known force to the mass of the instrument. Estimates of the system response of each channel, the response due to the instrument and signal conditioning, were obtained by minimizing the least squared error between the observed calibration pulses and pulses derived from theoretical models of the system. A typical response curve for a seismometer is shown in Figure 3 and the system parameters for each seismic channel are given in Table 1.

Table 1. Seismometer Response Characteristics

Channel	Sense	Natural Frequency (Hz)	Damping	Intrinsic Gain (V/mm/sec)
1	Vertical	1.096	0.775	172.5
2	Vertical	1.100	0.775	201.7
3	N-S	1.761	0.381	73.4
4	E-W	0.650	1.000	509.9

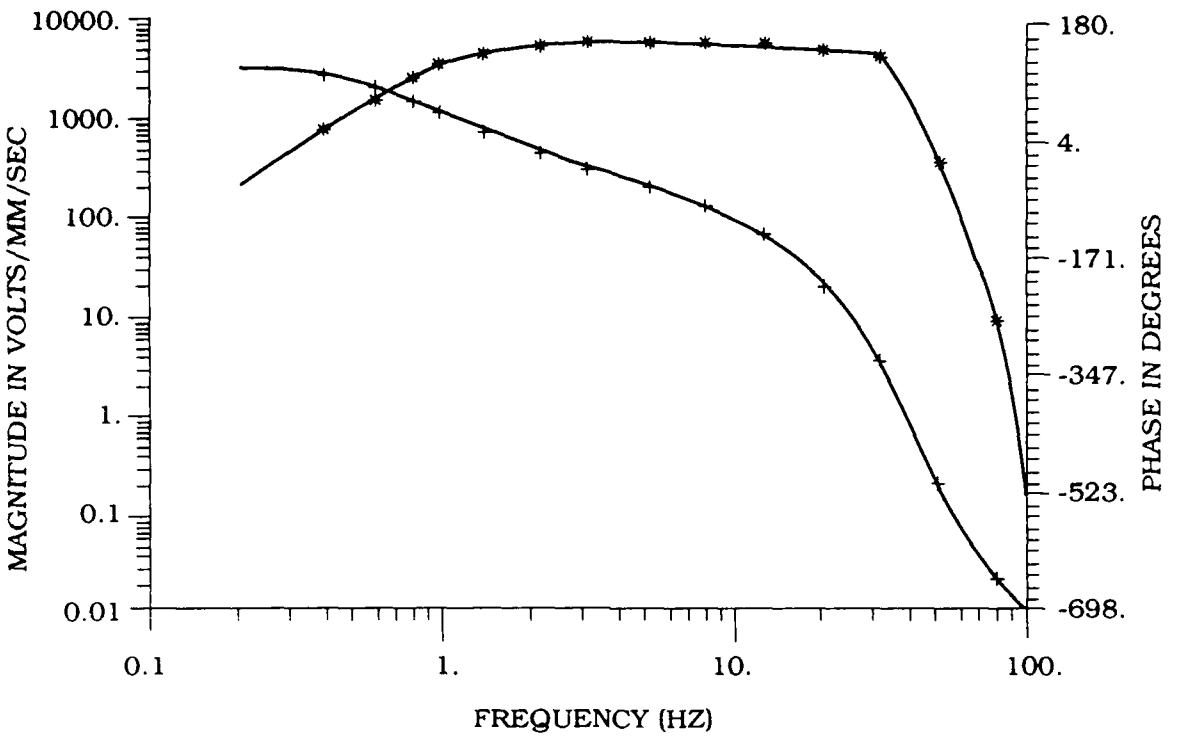

Figure 3. A Typical Seismometer Channel Response Curve From the La Junta Seismo-acoustic Array (Channel 1).

The design of the pressure transducers prevents *in-situ* calibration of the complete unit. Sensor scale factors were determined by loading each cell with a pressure defined by a column of water of known height. The electronic elements of the channel response are calibrated in the same manner as the seismic channel responses. Figure 4 shows a typical response curve for a pressure sensor and the channel response parameters are given in Table 2.

Table 2. Pressure Transducer Response Characteristics

Channel	Natural Frequency (Hz)	Time Constant (Sec)	Intrinsic Gain (V/mm/sec)
5	0.524	1.7	2.895
6	0.452	1.7	3.047
7	0.492	1.7	2.884

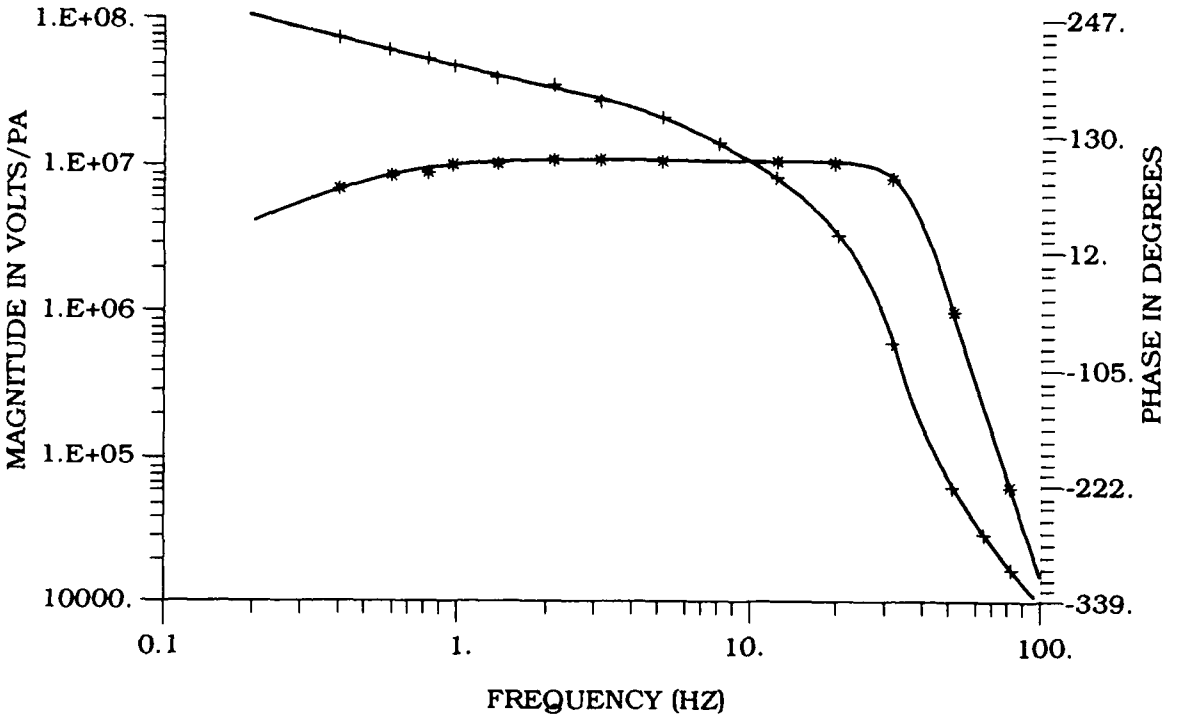

Figure 4. A Typical Pressure Sensor Channel Response Curve from the La Junta Seismo-acoustic Array (Channel 7).

4.3 System Measurement Errors

Any physically realizable measurement system will record, in addition to the desired signal, some level of noise. This noise can be external to the system and be introduced as an undesirable signal. In addition, the measurement system will introduce self-generated noise into the output signal. To insure the fidelity of the input and recorded signal, the system measurement errors must be significantly below the amplitude of the input signal.

4.3.1 ADDITIVE SYSTEM NOISE

An estimate of the additive system noise is made by comparing the outputs of two or more collocated sensors. The output of the jth channel, $s_j(t)$, is defined as:

$$s_j(t) = u_j(t) + N_j(t) \tag{1}$$

where $u_j(t)$ is that part of the signal due to sensor input and $N_j(t)$ is that part due to system measurement noise. For two collocated sensors, j and k, it is assumed that the sensor input term is common to both output channels while the system noise term is independent and incoherent across the channels, or:

$$u_j(t) = u_k(t) \tag{2}$$

and

$$\langle N_j(t) \cdot N_k(t) \rangle = \delta_{jk} \tag{3}$$

where $\langle x \cdot y \rangle$ denotes the inner product of x and y and δ_{jk} is the Kronecker delta function. Then, the system noise spectrum is defined as the output signal spectrum minus the coherent spectrum between collocated channels, i and j. Under this definition a lower bound estimate of the system noise will be made as any coherent noise terms are assumed to be part of the sensor input term.

The coherency function for channels i and j, $C_{ij}(f)$, is given by:

$$C_{ij}(f) = |G_{ij}(f)| / \left[G_{ii}(f) \cdot G_{jj}(f) \right]^{\frac{1}{2}} \tag{4}$$

where G_{ij} is the cross-spectral density function between channels i and j and G_{ii} is the auto-spectral density function for channel i. In turn, the incoherent noise spectrum is given by:

$$G^n_{jj}(f) = \left[1 - C_{ij}(f) \right] \cdot G_{jj}(f) \tag{5}$$

and is the basis for the estimate of the GDAS measurement system noise.

Figure 5 shows the average squared coherency function for the collocated vertical seismometers (channels 1 and 2 at the La Junta site). This estimate is based on data samples taken from all 67 available time windows. Figure 6 shows the equivalent function for two collocated pressure transducers (channels 5 and 6). A generally high level of coherency is seen between the vertical seismics in the band of approximately 15 to 35 Hz. For the pressure

transducers,, the coherency is much lower than for the seismic channels with the exception of a narrow band just above 10 Hz. Figures 7 and 8 give the incoherent spectral estimates between the respective sensors based on the 67 data segments. These plots represent the best lower bound estimates of additive system generated noise for seismic and pressure channels. The additive noise is approximately 4 to 6 orders of magnitude in power above the theoretical digitization noise, shown in Figure 9, of a 15-bit quantizer (A/D), as used in the GDAS.[3]

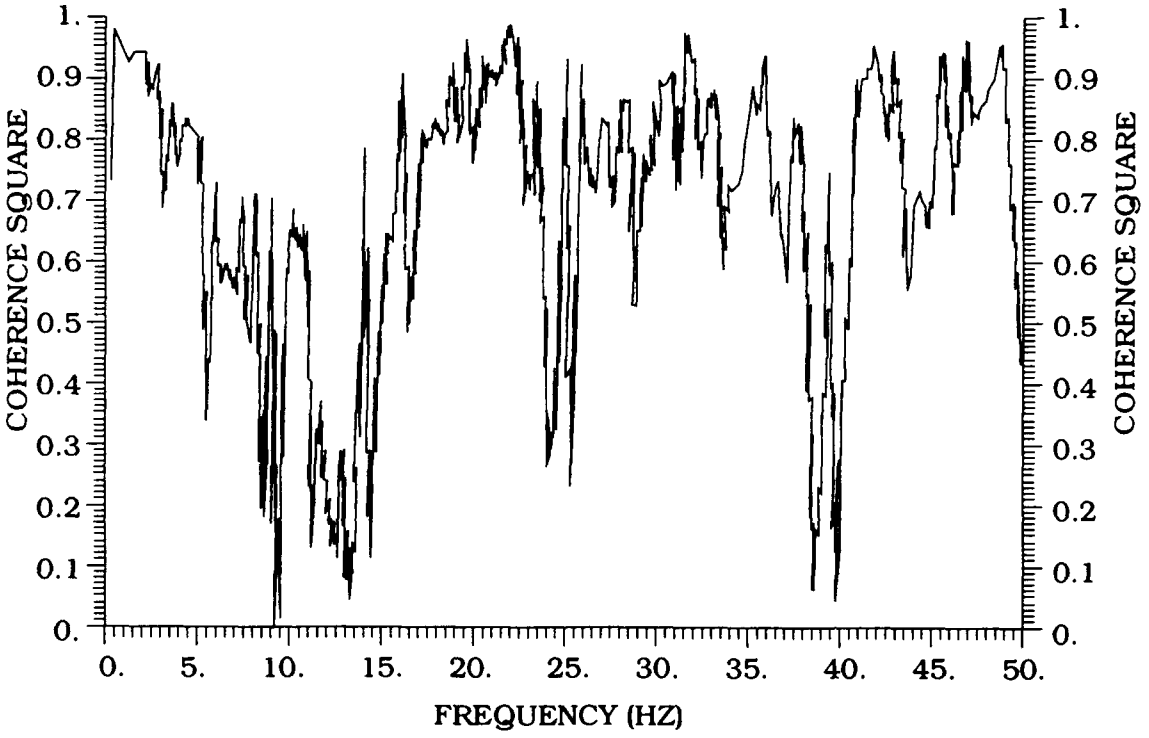

Figure 5. Average Squared Coherency Function for Two Collocated Vertical Seismometers from the La Junta Seismo-acoustic Array (Channels 1 and 2).

[3] Bennett, W. (1948) Spectra of Quantized Signals, *Bell Systems Technical Journal*, **27** (No. 3):446-472.

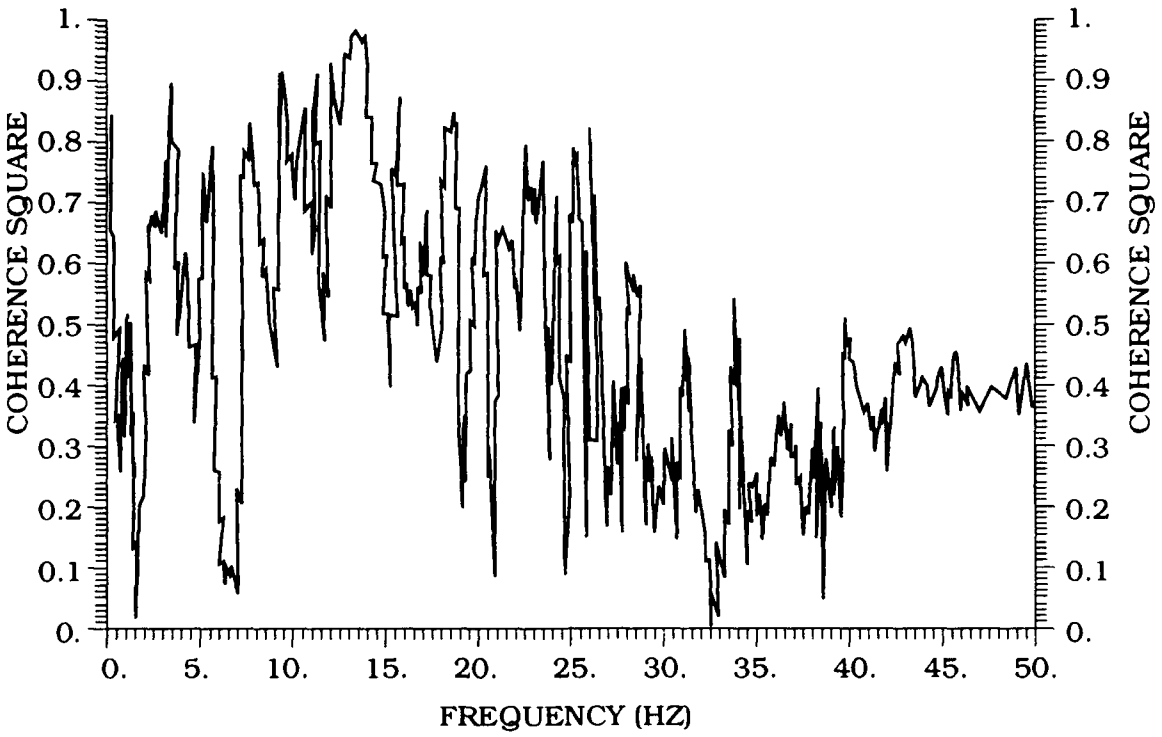

Figure 6. Average Squared Coherency Function for Two Collocated Pressure Transducers from the La Junta Seismo-acoustic Array (Channels 5 and 6).

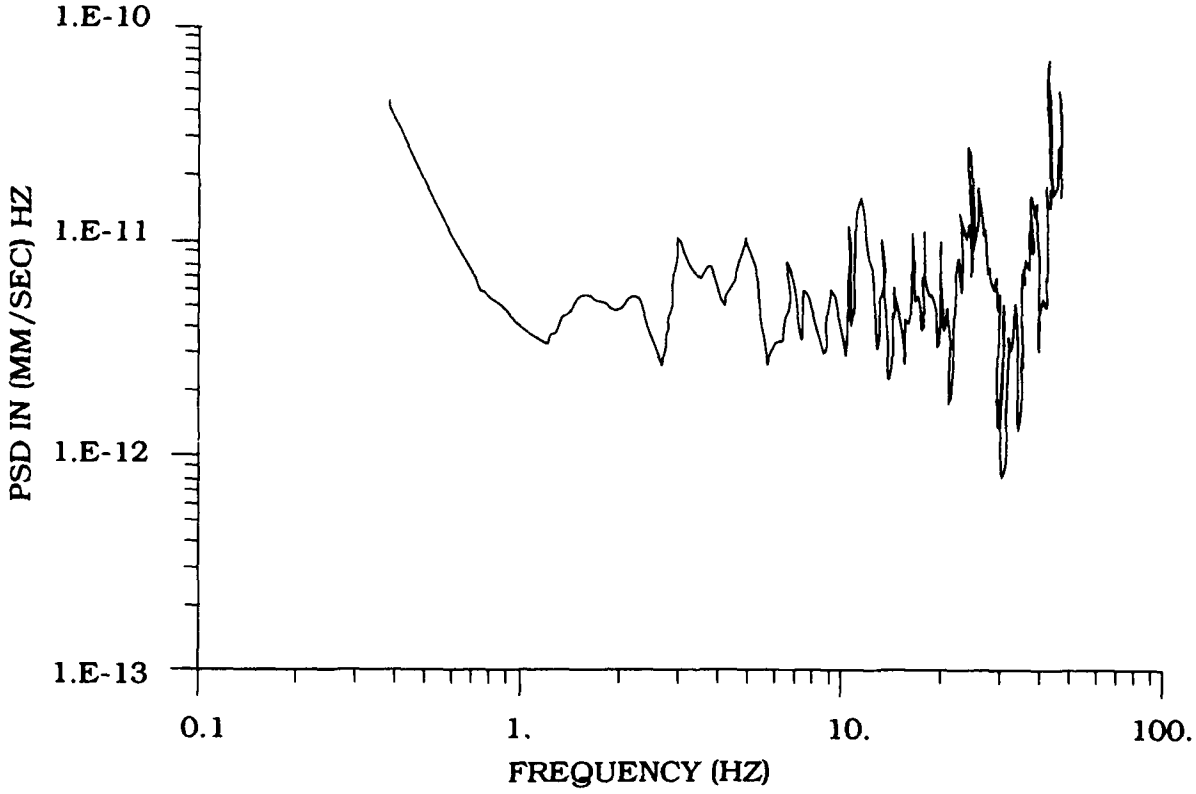

Figure 7. Average Incoherent Spectrum for Two Collocated Vertical Seismometers at the La Junta Seismo-acoustic Array (Channels 1 and 2).

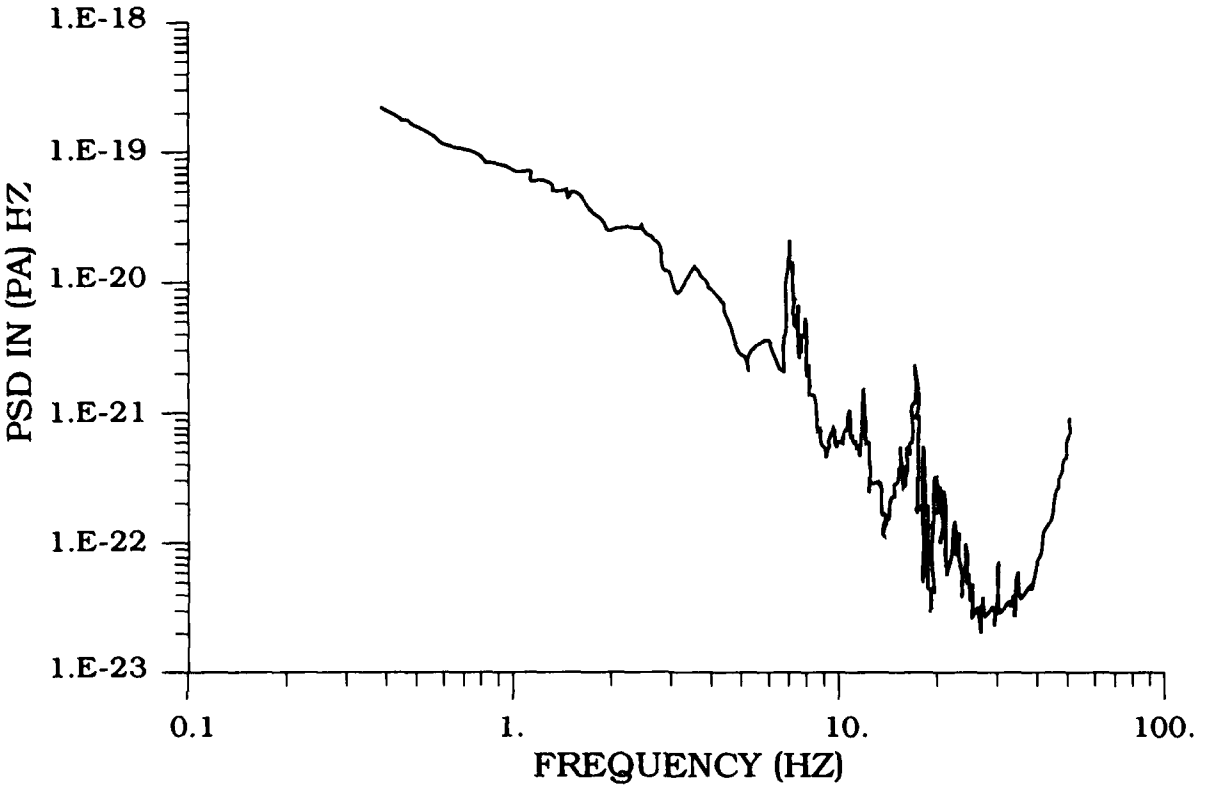

Figure 8. Average Incoherent Spectrum for Two Collocated Pressure Transducers at the La Junta Seismo-acoustic Array (Channels 5 and 6).

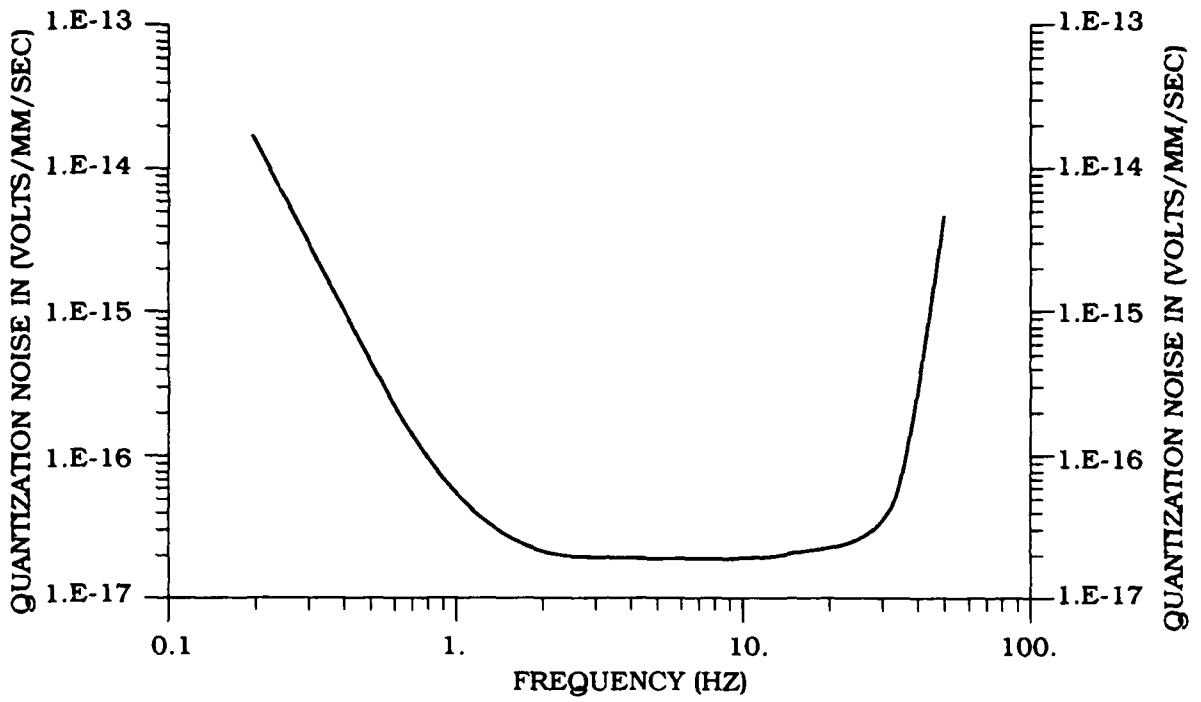

Figure 9. Theoretical Digitization Noise of a 15-bit Quantizer Representing the GDAS A/D System.

4.3.2 SIGNAL INDUCED NOISE

One potentially significant source of signal induced noise is the folding or aliasing of out-of-band power back into the measurement data band. The ability of the measurement system to mitigate this effect is characterized by the protection ratio, the ratio of the in-band system response to the response at the first fold-aliased frequency.[4] This can be expressed as:

$$P_i(f) = T_i(f)/T_i(f_S - f) \quad 0 < f < f_N \tag{6}$$

where $T_i(f)$ is the system response of channel i, f_S is the sampling frequency and f_N is the Nyquist frequency or $0.5f_S$. The protection ratio for channel 1, a vertical seismometer, is shown in Figure 10 and for channel 7, a pressure transducer, in Figure 11. Given equal amplitude inputs to the measurement system at some in-band frequency and its first fold

[4] Blackman, R., and Tukey, W. (1958) *The Measurement of Power Spectra*, Dover Publication, New York

frequency, the protection ratio is the relative amplitude of the in-band to the aliased signal at that frequency.

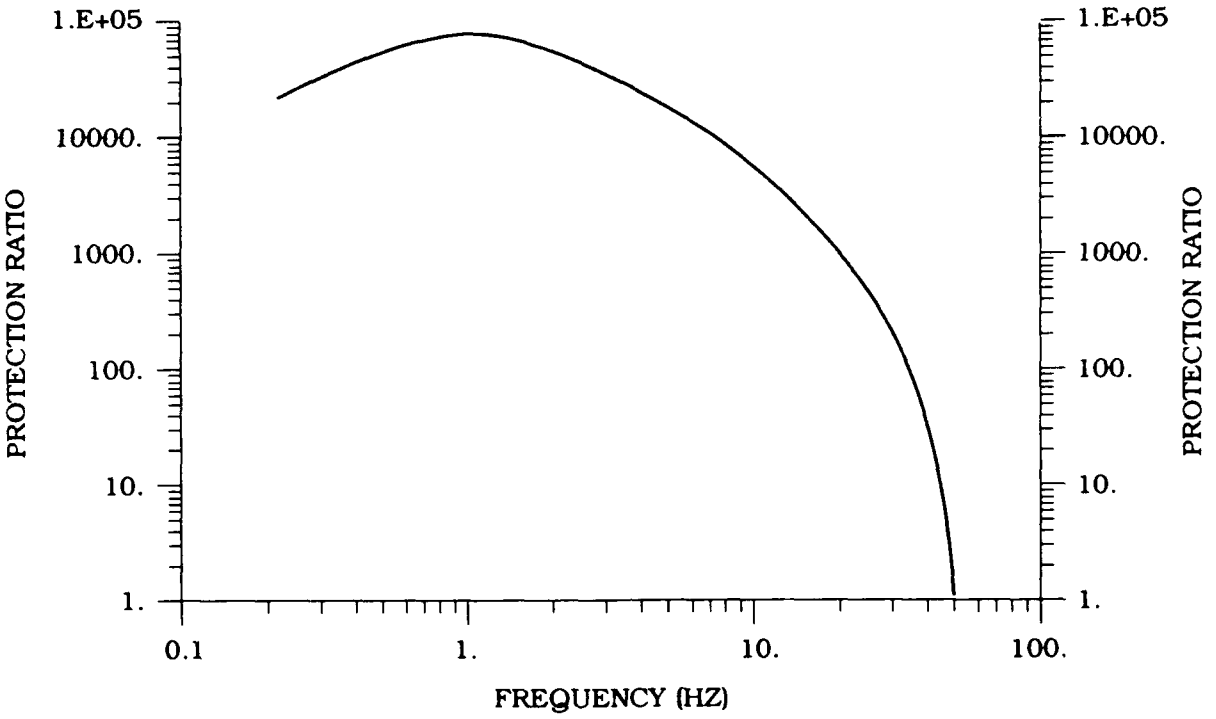

Figure 10. Protection Ratio for Channel 1, a Vertical Seismometer of the La Junta Seismo-acoustic Array.

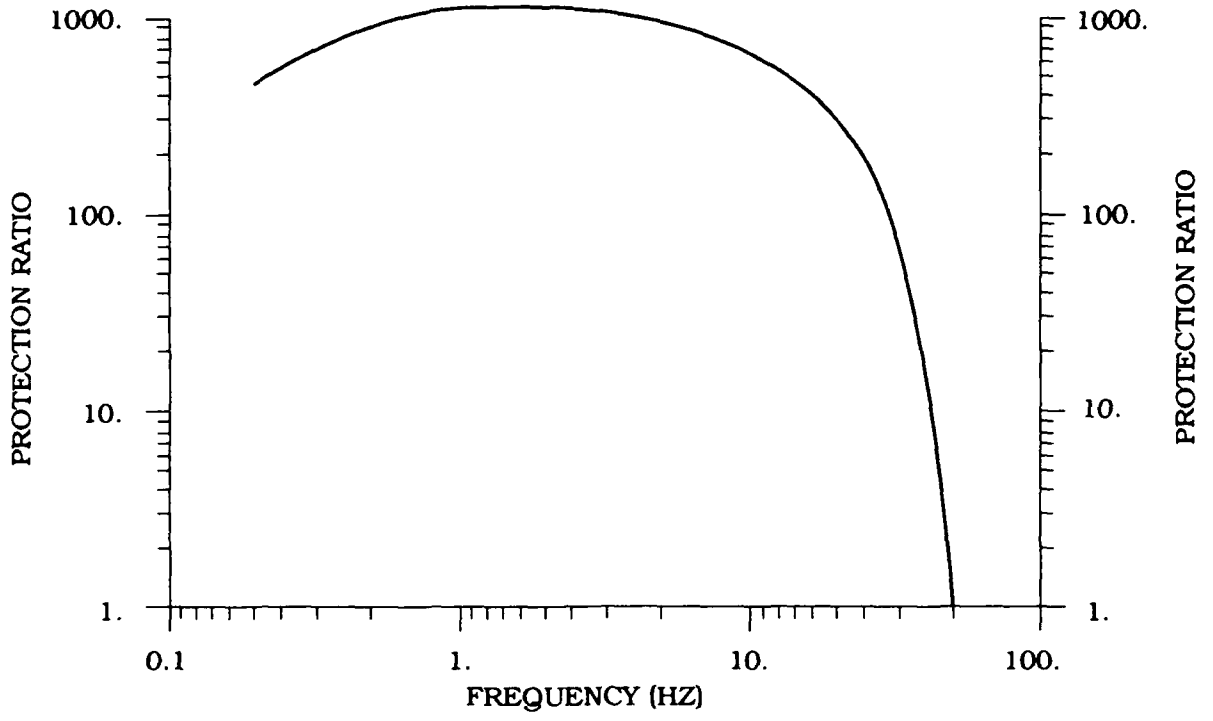

Figure 11. Protection Ratio for Channel 7, a Pressure Transducer of the La Junta Seismo-acoustic Array.

4.4 Data Quality

The quality of the data recorded at the La Junta array can be quantified in terms of the signal to noise ratio of the recordings. There are two potentially significant noise sources affecting the data, the additive systems noise and out-of-band signals. It is desirable to consider two forms of the signal to noise ratio to isolate the contribution of each noise source.

In Section 4.3.1, the signal was defined to be coherent across collocated sensors and the additive system noise was defined as the incoherent signal. Thus, the signal to noise ratio assuming only additive system noise is given by the ratio of the coherent spectra to the incoherent spectra for any given channel, or:

$$S/N_i = \left[G^s_{ii}(f)/G^n_{ii}(f) \right]^{\frac{1}{2}} \qquad (7)$$

or

$$S/N_i = \left[C_{ij}(f) / \left\{ 1 - C_{ij}(f) \right\} \right]^{\frac{1}{2}} \qquad (8)$$

for channel i. Figures 12 and 13 show the signal to noise ratios for vertical seismics and pressure transducers, respectively.

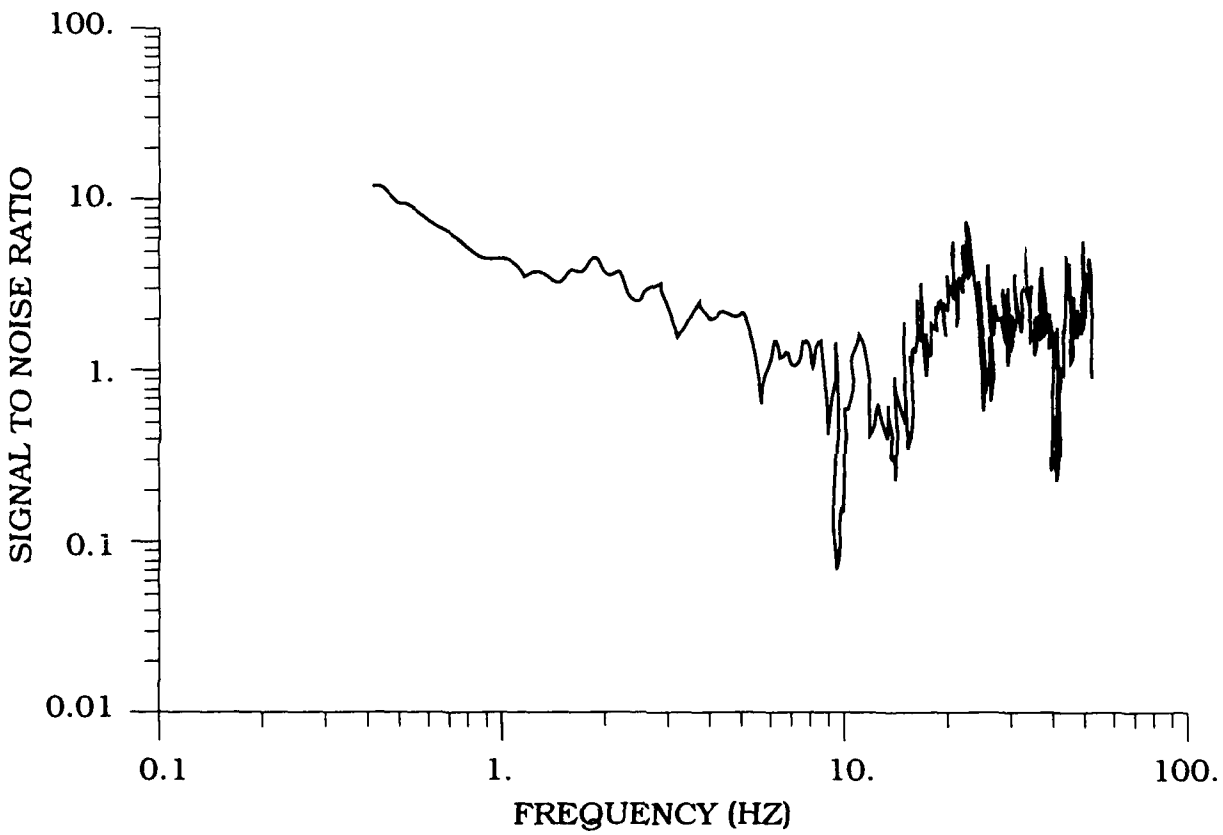

Figure 12. Signal to Noise Ratio (S/N) Assuming Only Additive System Noise for a Typical Seismic Channel Recording.

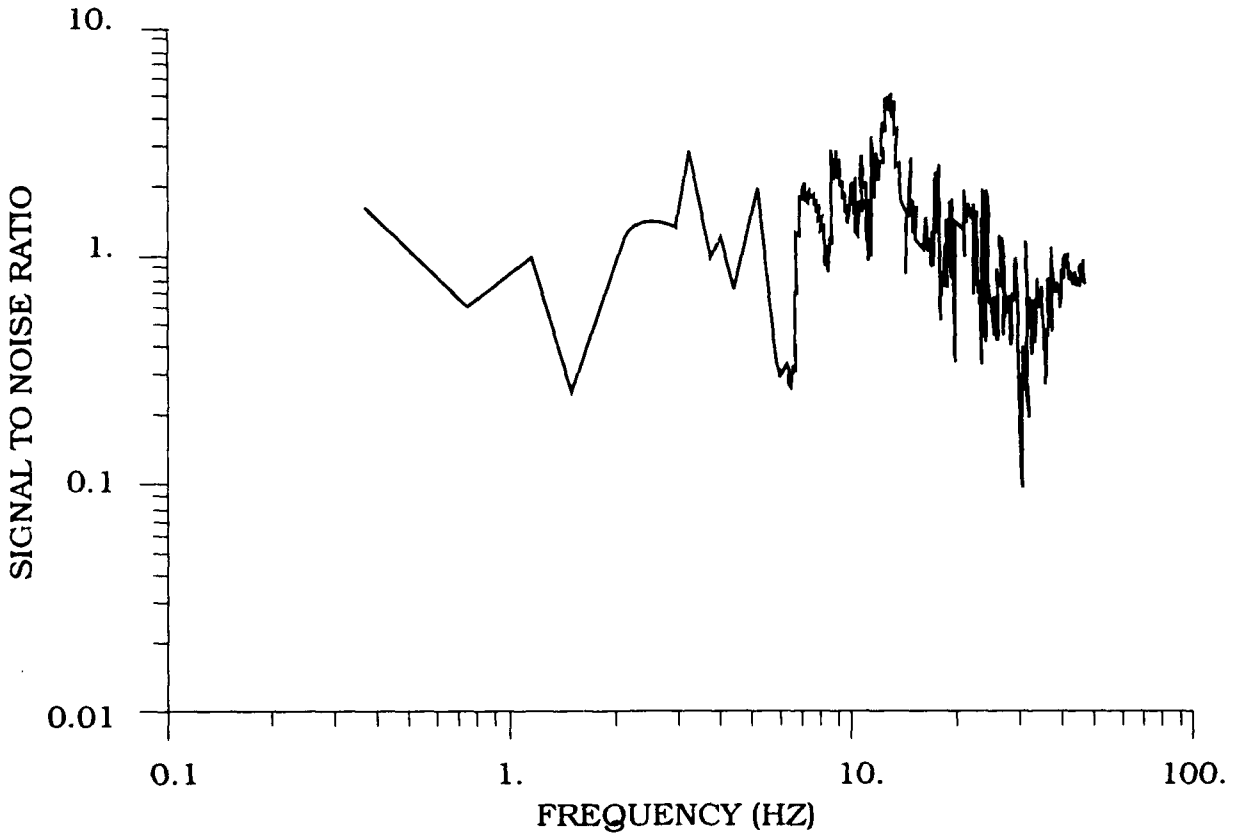

Figure 13. Signal to Noise Ratio (S/N) Assuming Only Additive System Noise for a Typical Pressure Channel Recording.

Alternatively, the signal to noise ratio can be described as the ratio of the maximum inband signal amplitude to the additive measurement noise plus the first fold aliasing error. This version of the signal to noise ratio is given by:

$$S/N'_i = \left[G^s_{ii}(f) / \left\{ G^n_{ii}(f) + G^s_{ii}(f_N) \cdot p_i^{-2}(f) \right\} \right]^{\frac{1}{2}} \tag{9}$$

where $G^{si}{}_i(f_N)$ is the maximum coherent signal power at the Nyquist frequency, f_N. No significant differences were noted between the two definitions of signal to noise. This indicates that the inband signals are not being distorted by aliasing of power from outside the measurement band.

5. SEISMO-ACOUSTIC NOISE ENVIRONMENT

5.1 Introduction

Seismic noise at any site, particularly for shallow instruments, can generally be characterized as a combination of weak propagating disturbances from distant and near sources often associated with cultural activity and meteorological conditions. Pressure noise results from the pressure fluctuations due to turbulent motions within the atmosphere, that is, wind generated noise. It is well known that these noise fields demonstrate strong seasonal and daily variation due primarily to meteorological effects.[5, 6] It was the goal of this study to evaluate parameters to describe the statistical character of the noise fields observed at the La Junta array and to establish the degree of correlation between the pressure and seismic noise signals.

5.2 Broadband Characteristics

During the period 9 through 29 October 1986, the La Junta seismo-acoustic array was triggered every 5 hours to obtain 30-sec segments of data at 100 samples/sec. A total of 74 data segments were collected during this window. The raw data files were reviewed and 5.12-sec samples selected for processing to eliminate data either demonstrating equipment malfunctions or containing apparent discrete transient events. Of the original 73 data segments, 67 segments were used for analysis. Figure 14 shows typical examples of the seismic and pressure noise data as recorded at the La Junta array.

Overall standard deviations for each channel were 2.94×10^{-5} and 8.61×10^{-5} mm/sec for the vertical and horizontal seismic components, respectively, and 1.96×10^{-1} Pa for the atmospheric pressure noise. Figure 15 displays the cumulative probability distribution functions, plotted on normal probability scales, of the vertical and horizontal seismic and pressure noise amplitudes. The strong divergence from linear behavior in the tails of the distributions demonstrates the non-Gaussian nature of the broadband seismic and pressure noise fields. The non-Gaussian behavior of the data is attributed to non-stationarity of the distribution parameters.

---

[5] Aki, K., and Richards, P. (1980) *Quantitative Seismology: Theory and Methods*, W. H. Freeman and Company, San Francisco.

[6] Ringdal, F., and Bungum, H. (1977) Noise level variation at NORSAR and its effect on detectability, *Bull. Seism. Soc. Amer.*, **67**(No. 2):479-492.

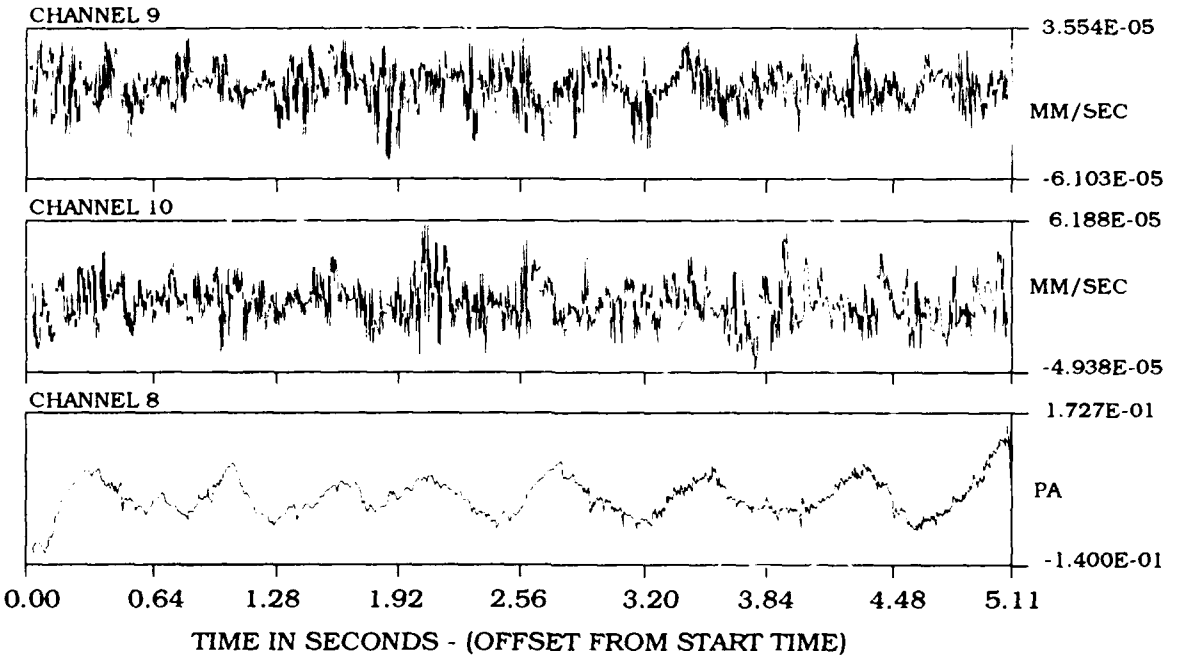

Figure 14. Typical Noise Signals for Vertical (Upper) and Horizontal (Middle) Seismics and a Pressure (Lower) Transducer Channels.

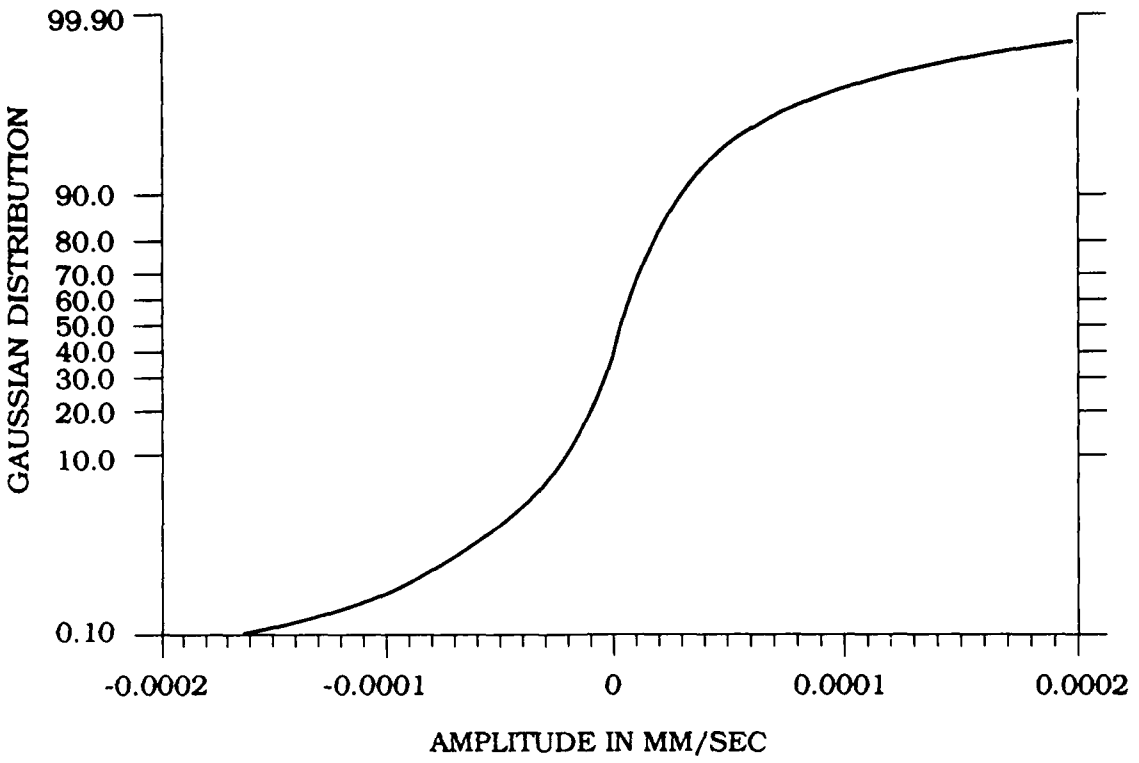
99.90
90.0
80.0
70.0
60.0
50.0
40.0
30.0
20.0
10.0
0.10
GAUSSIAN DISTRIBUTION
-0.0002
-0.0001
0
0.0001
0.0002
AMPLITUDE IN MM/SEC

Figure 15a.

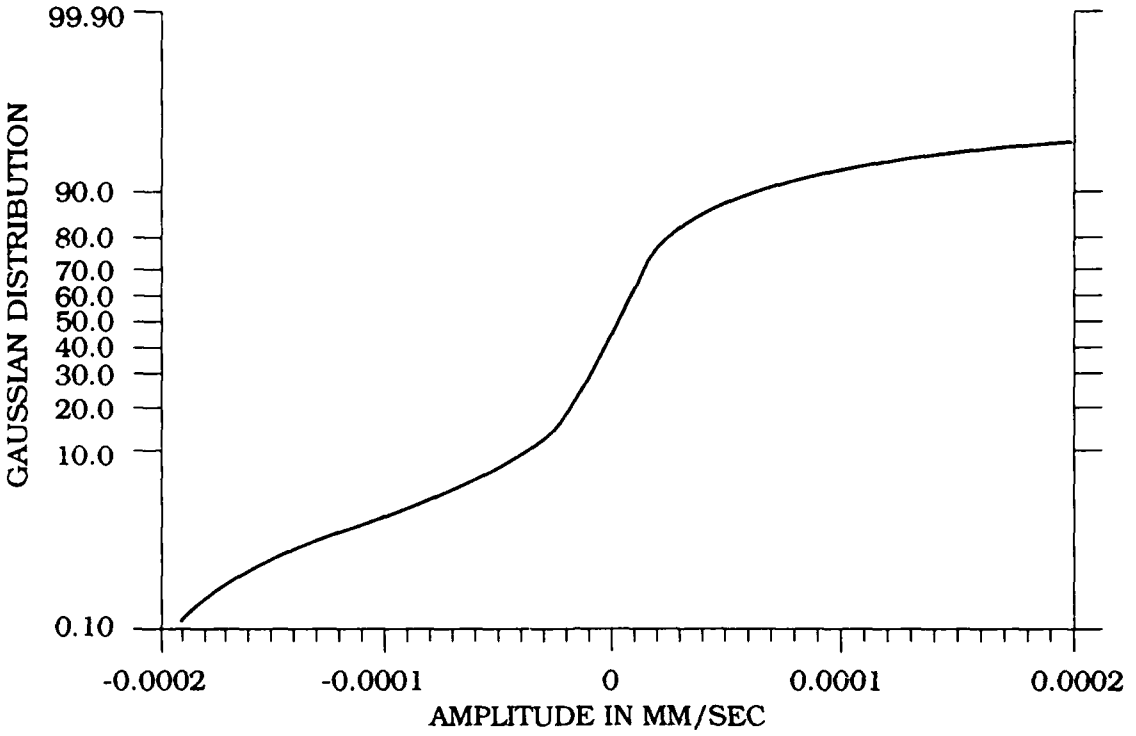
99.90
90.0
80.0
70.0
60.0
50.0
40.0
30.0
20.0
10.0
0.10
GAUSSIAN DISTRIBUTION
-0.0002
-0.0001
0
0.0001
0.0002
AMPLITUDE IN MM/SEC

Figure 15b.

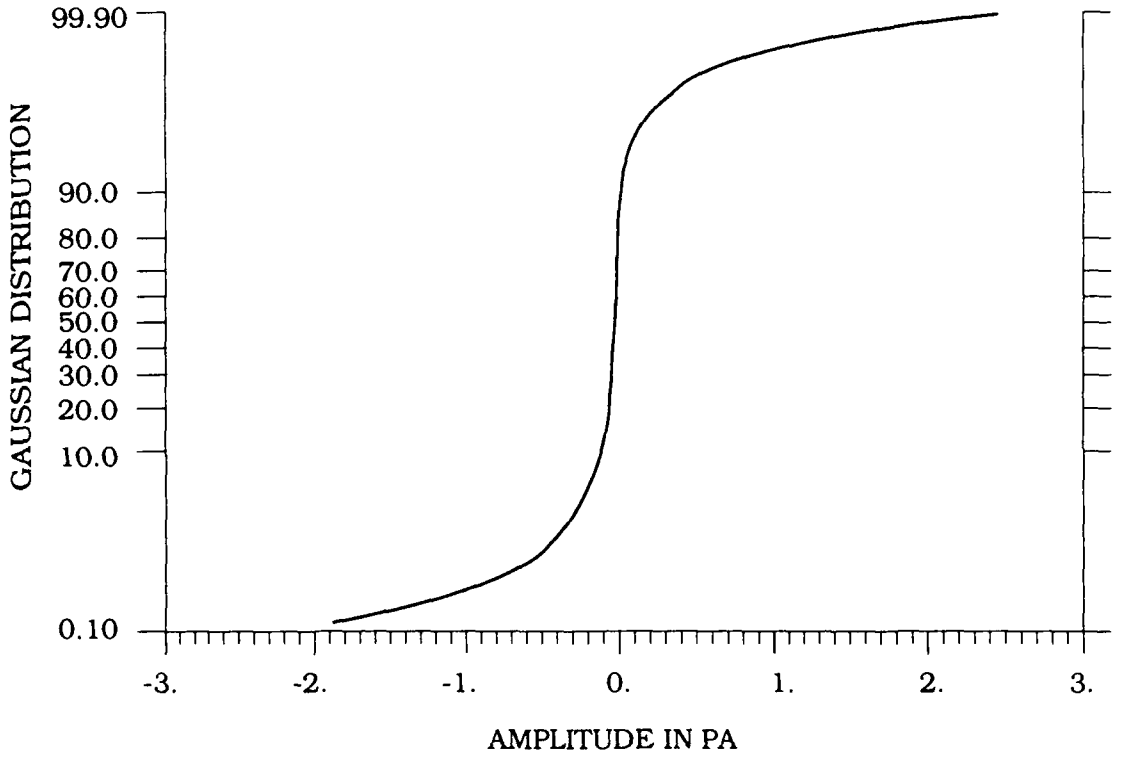

Figure 15c.

Figure 15. Cummulative Probability Distributions for Vertical (a), and Horizontal (b) Seismic and Pressure (c) Noise Amplitude Data on a Normal Probability Scale.

In addition to the Gaussian distribution, the data was compared to the Gumbel Type II extreme-value distribution. Distribution parameters were obtained based on the observed maximum absolute value of each measured field in 1.01-sec windows. The parameters of these distributions are [$u = 3.8 \times 10^{-5}$, $K = 2.56$] and [$u = 9.1 \times 10^{-5}$, $K = 2.29$] for vertical and horizontal seismics, respectively, and [$u = 0.108$, $K = 2.12$] for the atmospheric pressure field. The observed and theoretically estimated distribution functions are shown in Figure 16. While the estimated functions are not perfect representations of the observed distributions, vertical seismic and pressure distributions are considered to be adequately fit.

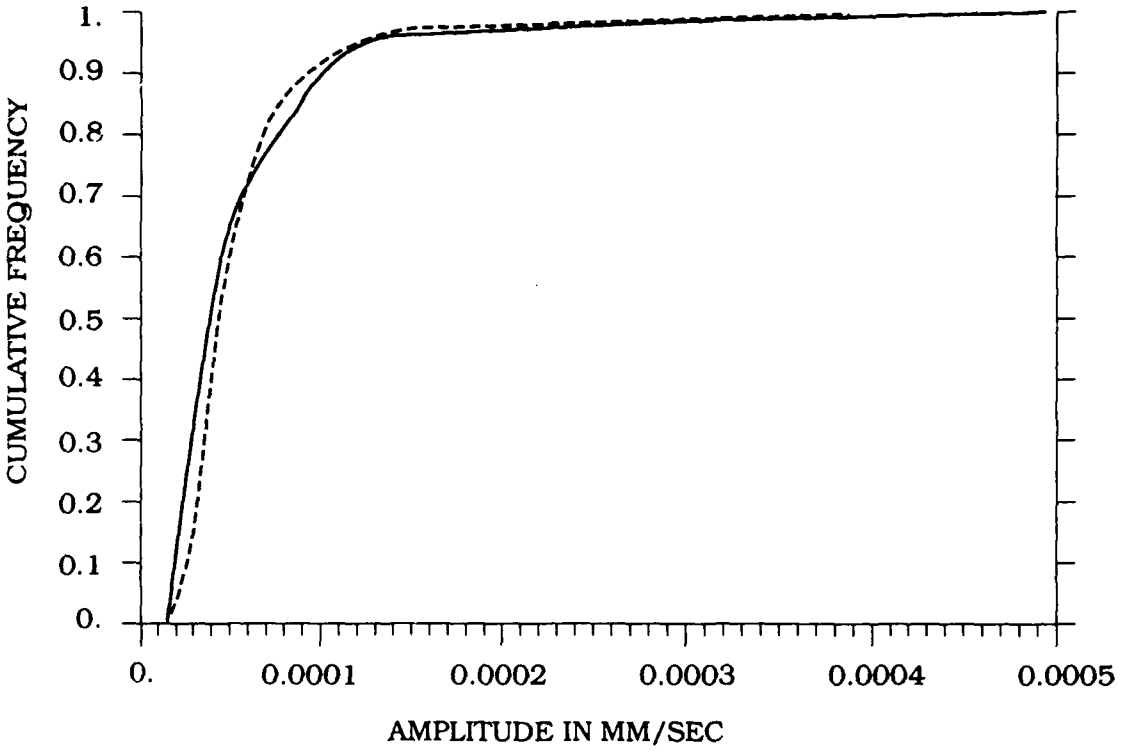
CUMULATIVE FREQUENCY
1.
0.9
0.8
0.7
0.6
0.5
0.4
0.3
0.2
0.1
0.
0.
0.0001
0.0002
0.0003
0.0004
0.0005
AMPLITUDE IN MM/SEC

Figure 16a.

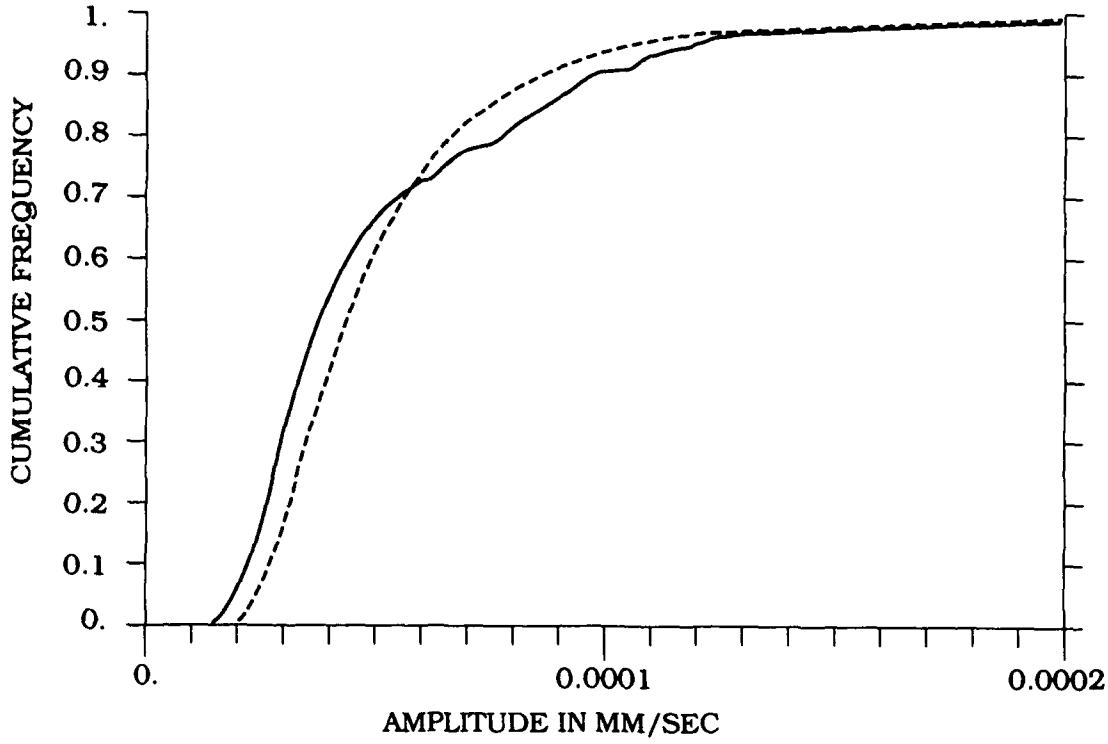
1.
0.9
0.8
0.7
0.6
0.5
0.4
0.3
0.2
0.1
0.
CUMULATIVE FREQUENCY
0.
0.0001
0.0002
AMPLITUDE IN MM/SEC

Figure 16b.

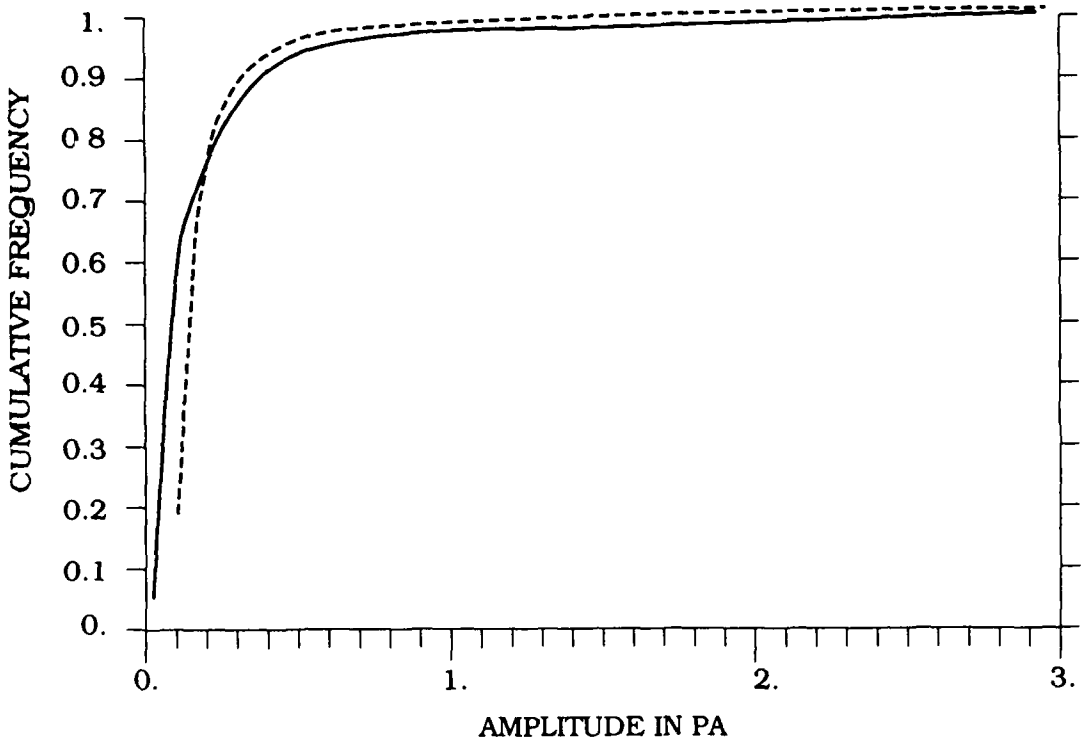

Figure 16c.

Figure 16. Observed (Solid) and Fit (Dashed) Gumbel Type II Extreme Value Distributions for (a) the Vertical Seismic Noise, (b) Horizontal Seismic Noise, and (c) the Atmospheric Pressure Signal.

Figures 17 through 19 summarize the temporal variation of maximum magnitude, the largest absolute value of the signal amplitude and the sample standard deviation for the vertical and horizontal components of seismic motion and a pressure channel during the observation period. Each vertical bar on the plots represents the value obtained from one 5.12-sec data sample with a 5-hour time shift between sequential bars. The cross-hatched bars fill for samples that were eliminated from analysis due to apparent equipment failures or obvious transient events.

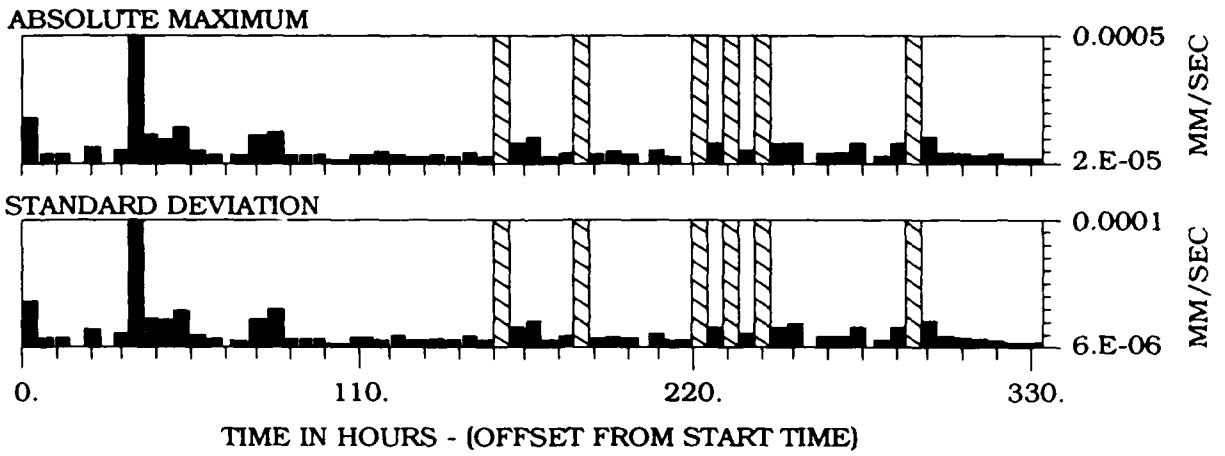

Figure 17. Amplitude Statistics of the Vertical Seismic Noise Field at 5-Hour Intervals.

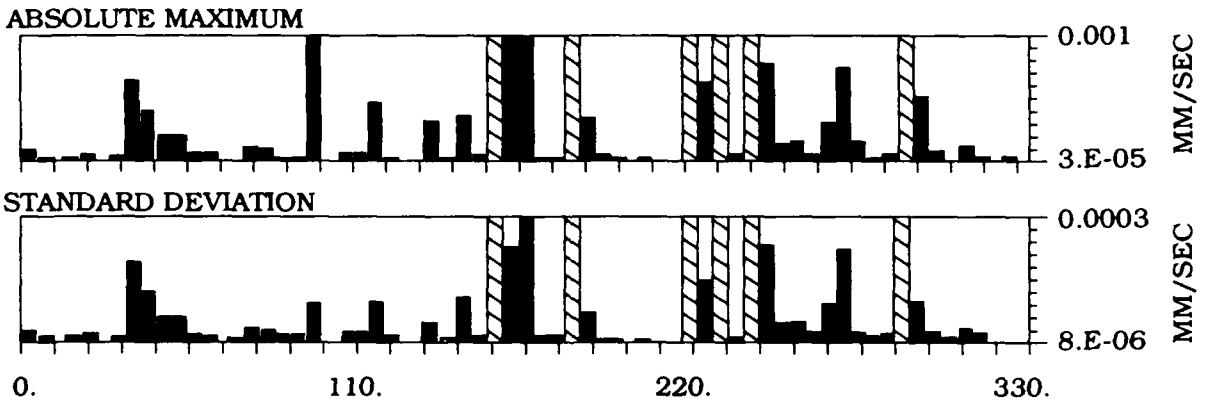

Figure 18. Amplitude Statistics of the Horizontal Seismic Noise Field at 5-Hour Intervals.

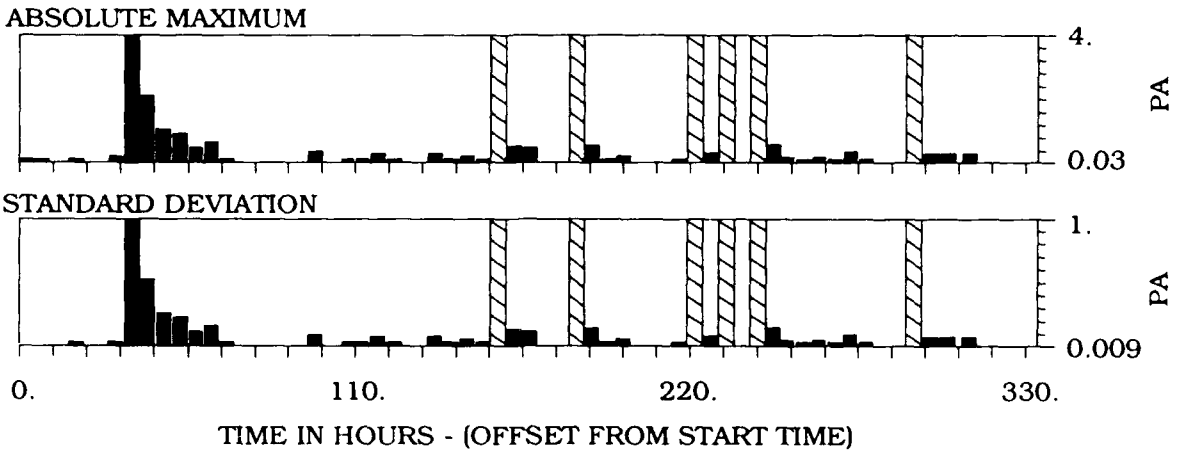

Figure 19. Amplitude Statistics of the Pressure Noise Field at 5-Hour Intervals.

Considering each plot separately, it is seen that the maximum magnitude and the standard deviation on each plot move essentially in lock step. In other words, increases in maximum magnitude are associated with increases in the general level of the noise and are not the result of the injection of isolated spikes within an essentially constant background.

Contrasting the figures, it is apparent that there is some degree of correlation between the pressure noise and surficial noise levels and that this correlation is most prominent during the period between 30 and 60 hours into the sampling window. The strength of the correlation during this period is emphasized due to the extremely high pressure noise level observed which, in turn, de-emphasizes the variation in pressure noise levels at other times. While a careful examination of the data outside this window shows correlation between periods of high seismic and pressure noise, it is also apparent that it is not strong. similarly, a general correlation can be seen between the vertical and horizontal component of the seismic noise. As is often found for seismic noise, however, the vertical component demonstrates a smaller degree of variation than do the horizontal motions.[5]

Figure 20 is a polar plot of the relative frequency of the azimuth of particle motion in the horizontal plane based on azimuth estimates from all 67 data segments in the analysis. It is apparent from this plot that the horizontal particle motion distribution is non-isotropic and is biased along an axis between NE-SW and E-W, approximately 80°-260°. No further attempt was made to identify the cause or in any other way examine this feature of the seismic noise field.

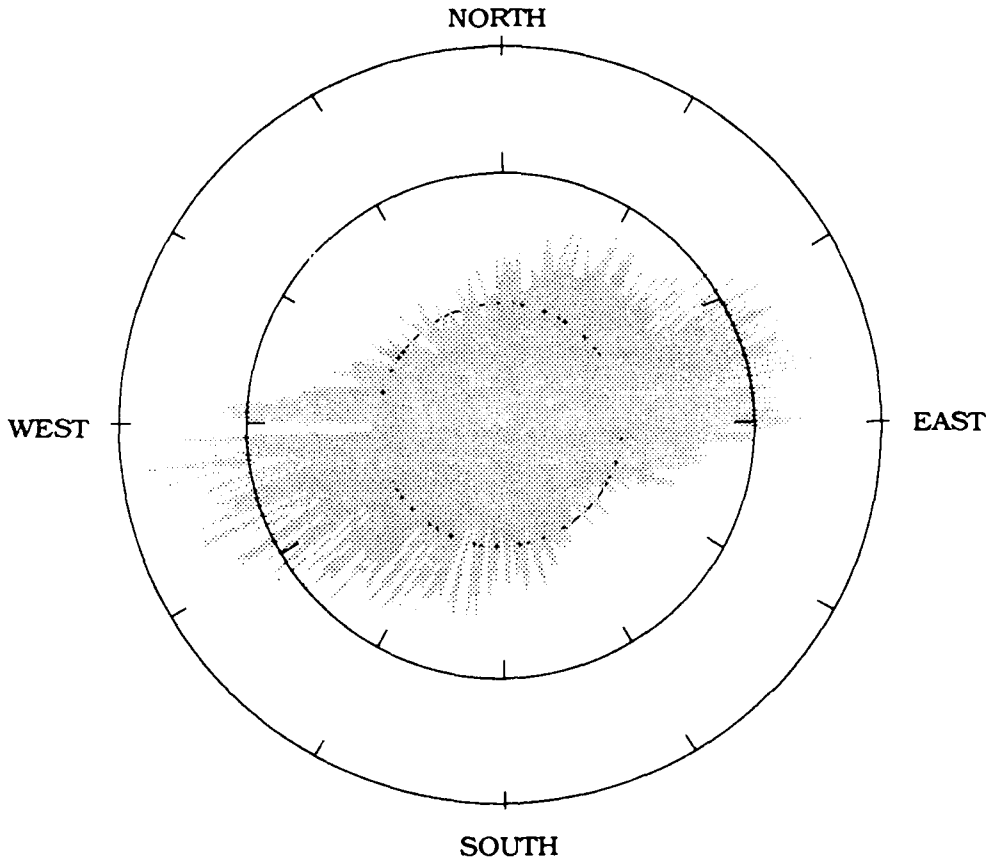

Figure 20. Relative Frequency of Horizontal Particle Motions Recorded at the La Junta Site.

5.3 Spectral Characterization

Mean periodograms evaluated for vertical and horizontal seismics and pressure noise data using the ensemble of sample segments are shown in Figure 21. The pressure periodogram shows a typical, nearly linear, wind noise roll off out to the anti-aliasing filter cut-off frequency of 30 Hz.[7] At low frequencies, below approximately 1 Hz, the seismic periodograms show significant power commonly associated with the storm microseism.

---

[7] Bruce, R. (1971) Field measurements: equipment and techniques, in *Noise and Vibration Control*, L. Beranek, ed., McGraw-Hill Book Company, New York.

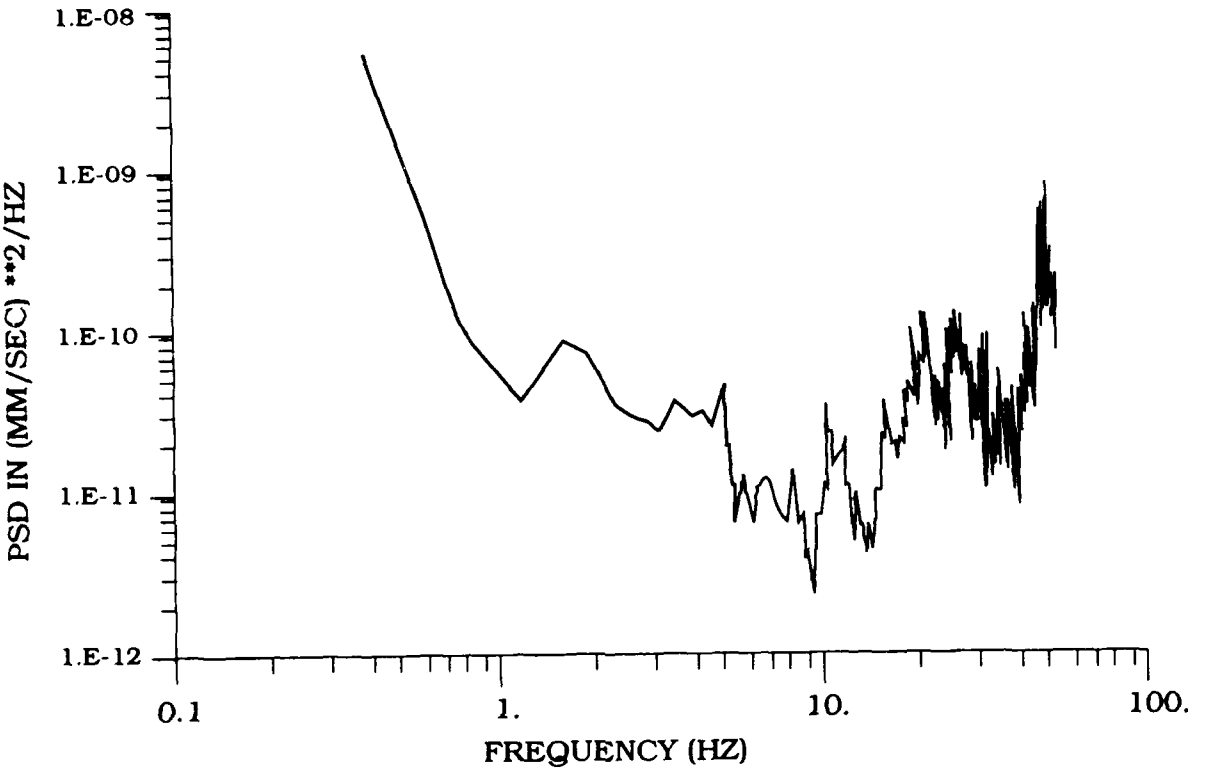
1.E-08
1.E-09
1.E-10
1.E-11
1.E-12
PSD IN (MM/SEC) **2/HZ
0.1
1.
10.
100.
FREQUENCY (HZ)

Figure 21a.

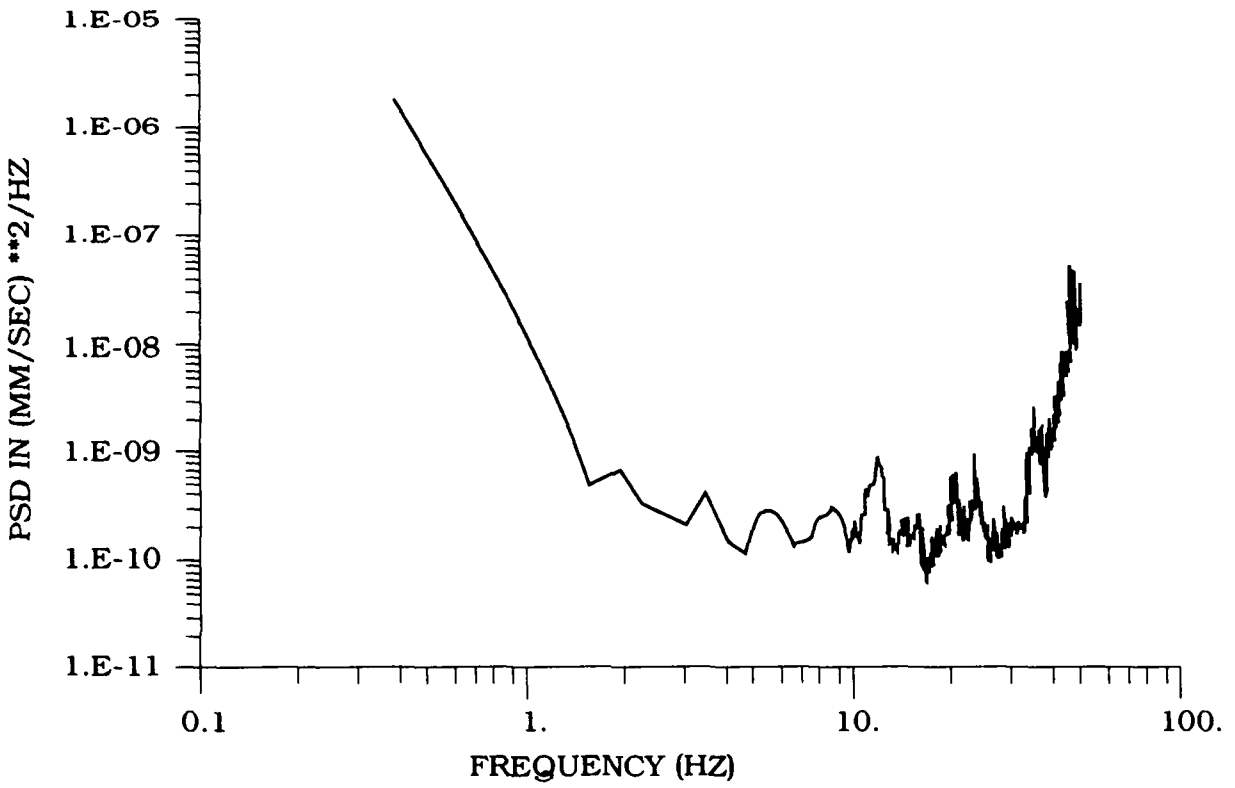
1.E-05
1.E-06
1.E-07
1.E-08
1.E-09
1.E-10
1.E-11
PSD IN (MM/SEC) **2/HZ
0.1
1.
10.
100.
FREQUENCY (HZ)

Figure 21b.

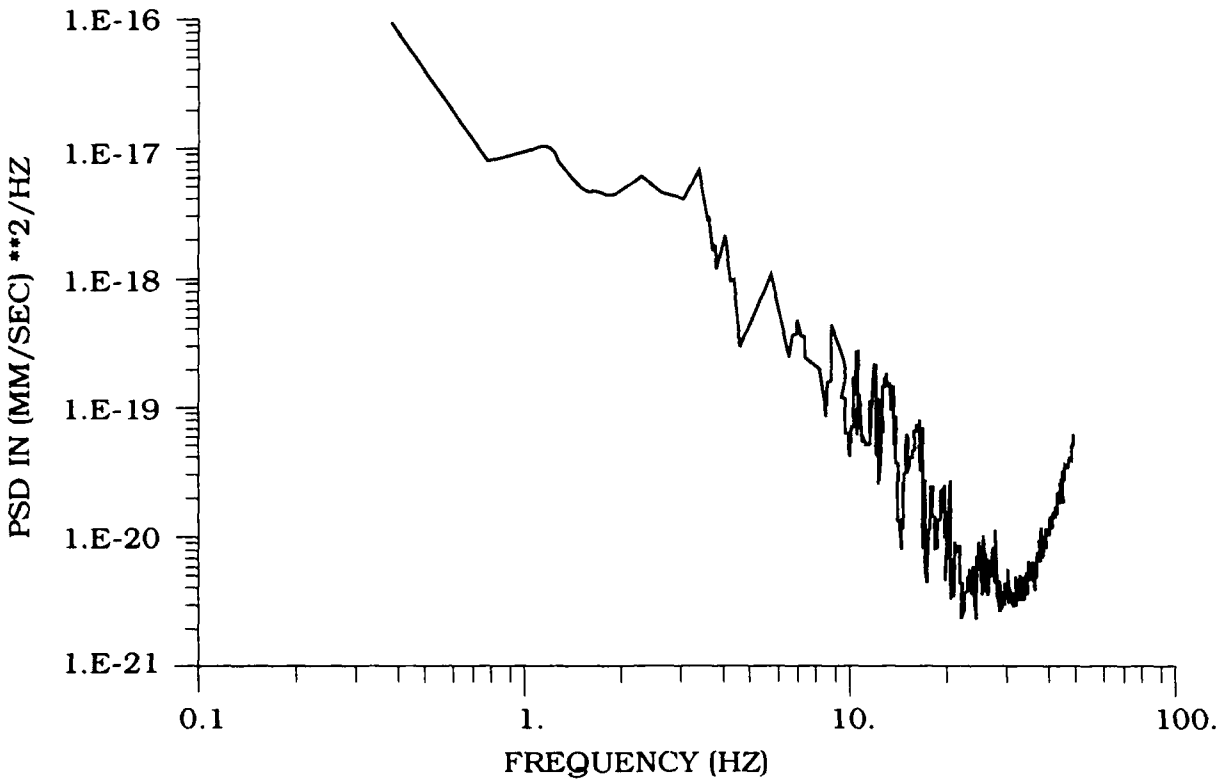

Figure 21c.

Figure 21. Mean Periodograms of the Vertical (a) and Horizontal (b) Seismic and Pressure (c) Noise Data.

As was demonstrated in Section 5.2, the broadband seismic and pressure noise field cannot be described as Gaussian. However, that does not preclude the possibility that within specific spectral bands the fields are Gaussian. The hypothesis that the noise fields, within narrow bands, is Gaussian can be tested using a technique proposed by Sax.[8] This test is based on the fact that periodogram coefficients for a stationary, Gaussian process are distributed as a Rayleigh process. Then, if the observed coefficients are plotted against a Rayleigh distribution, a straight line fit of the coefficients should be observed.

Figure 22 shows examples of the test results for the vertical and horizontal seismics and the pressure data for a band centered at a frequency of 5.1 Hz. In this case, as for all other frequencies tested, the results are distinctly non-linear and do not support an assumption of an active Gaussian process.

---

[8] Sax, R. (1968) Stationarity of seismic noise, *Geophysics*, **33** (No. 4):668-674.

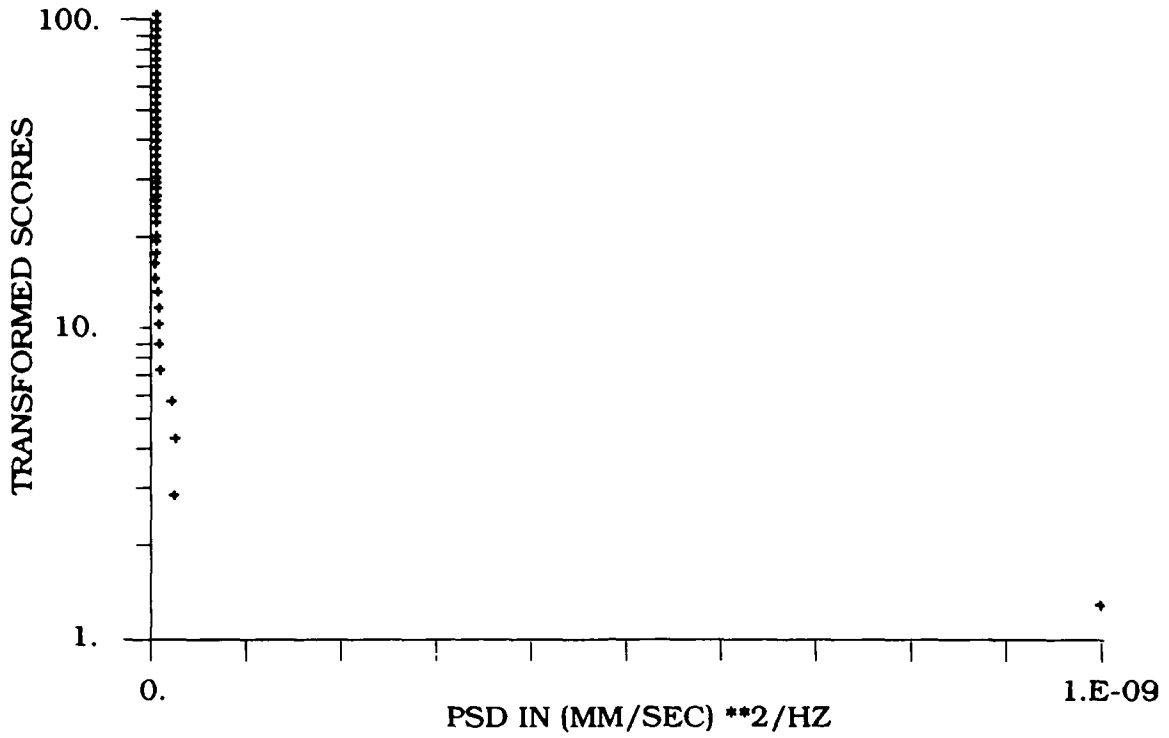

Figure 22a.

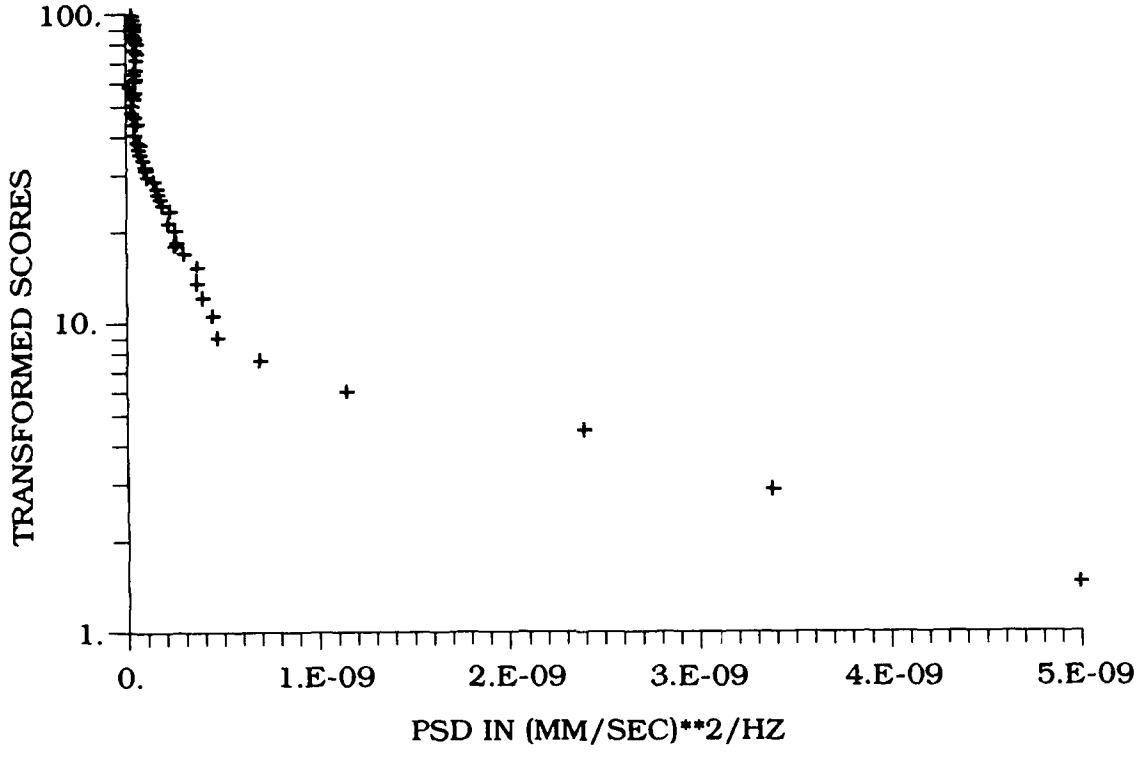
100.
10.
1.
TRANSFORMED SCORES
0.
1.E-09
2.E-09
3.E-09
4.E-09
5.E-09
PSD IN (MM/SEC)**2/HZ

Figure 22b.

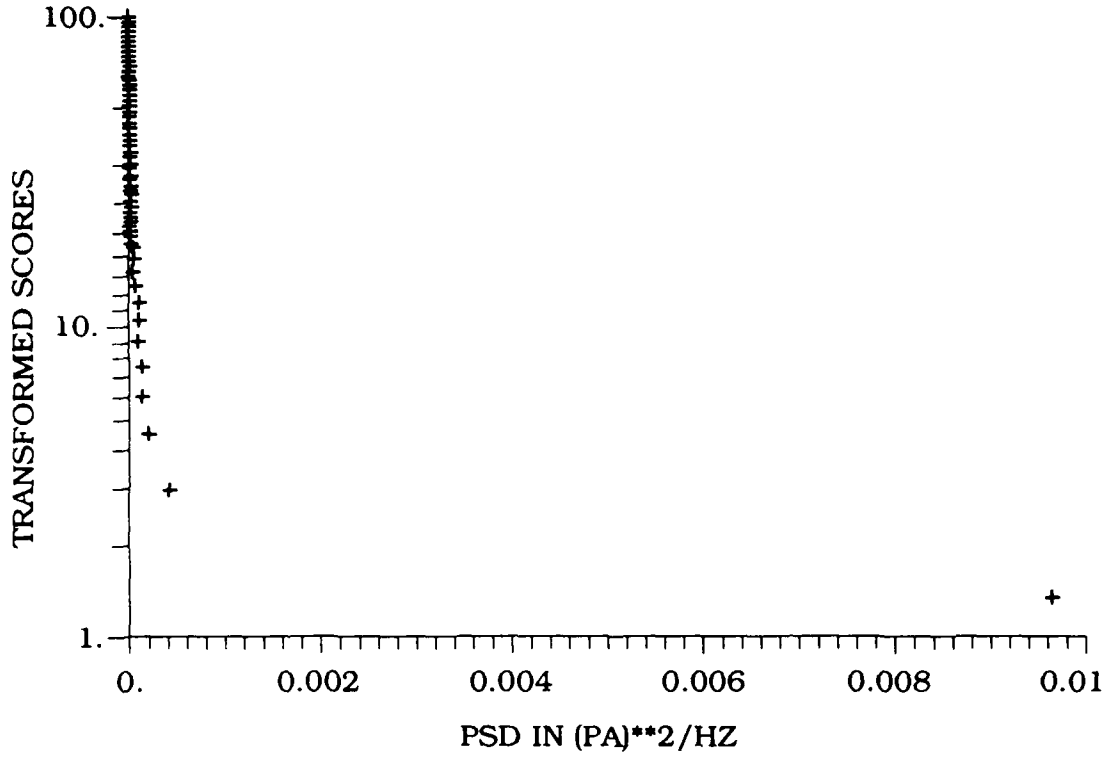

Figure 22c.

Figure 22. Distribution of Periodogram Coefficients at 5.1 Hz Versus a Rayleigh Distribution for Vertical (a) and Horizontal (b) Seismic, and Pressure (c) Noise.

5.4 Cross-Field Coherency

Figures 23 through 25 show the coherency squared function across noise fields, specifically between vertical and horizontal seismics, vertical seismics and pressure and horizontal seismics and pressure. In contrast to the like field coherencies, such as shown in Figure 5 for two vertical seismometers, only very weak coherencies, at best, are found across fields.

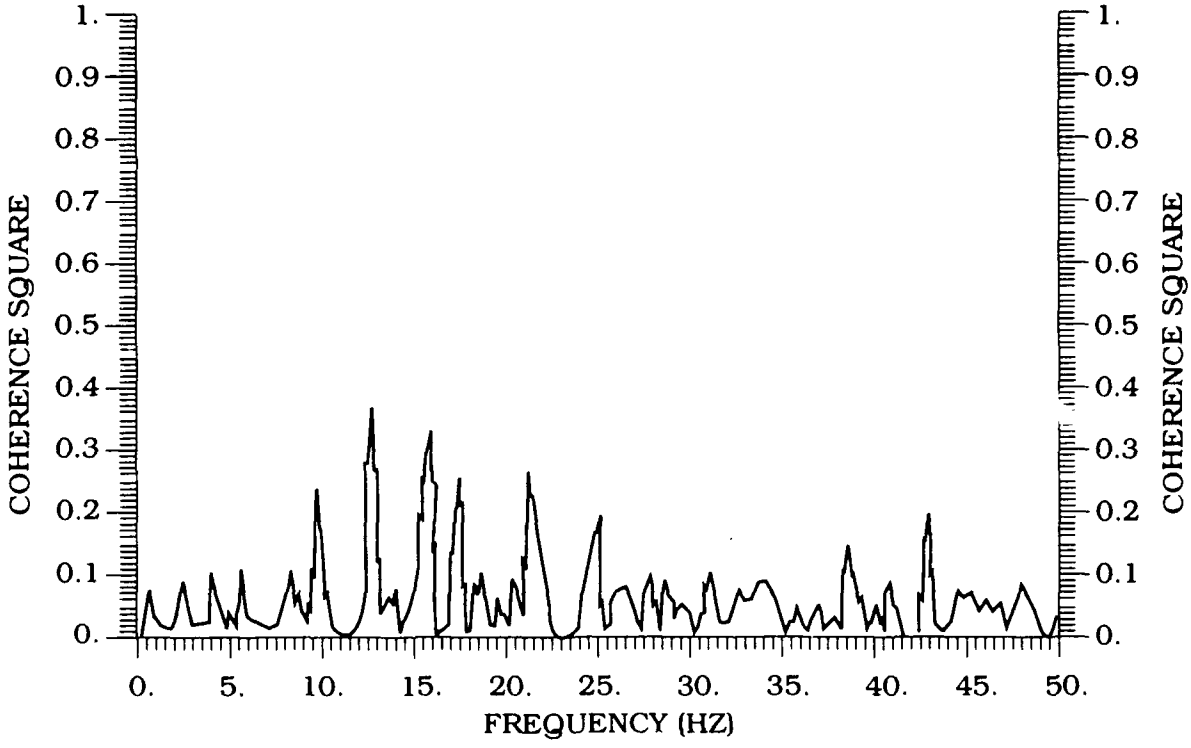

Figure 23. Coherency Squared Function Between Vertical and Horizontal Seismic Noise.

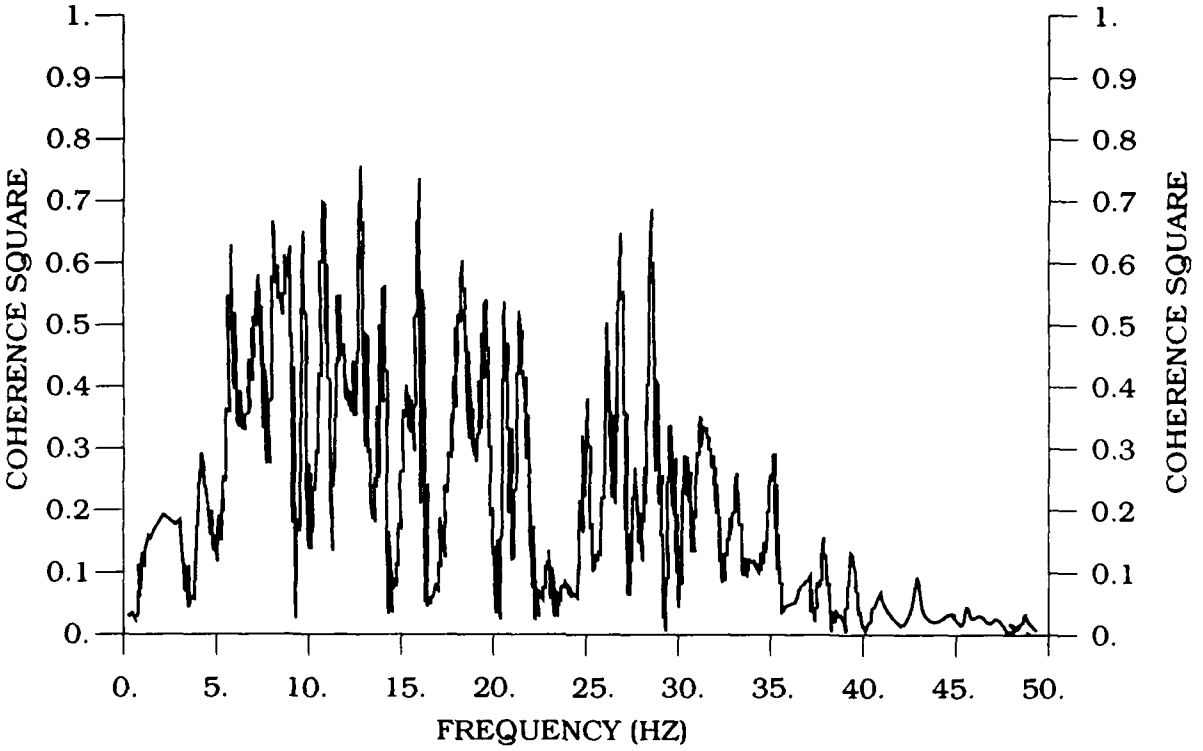

Figure 24. Coherency Squared Function Between Vertical Seismic and Pressure Noise.

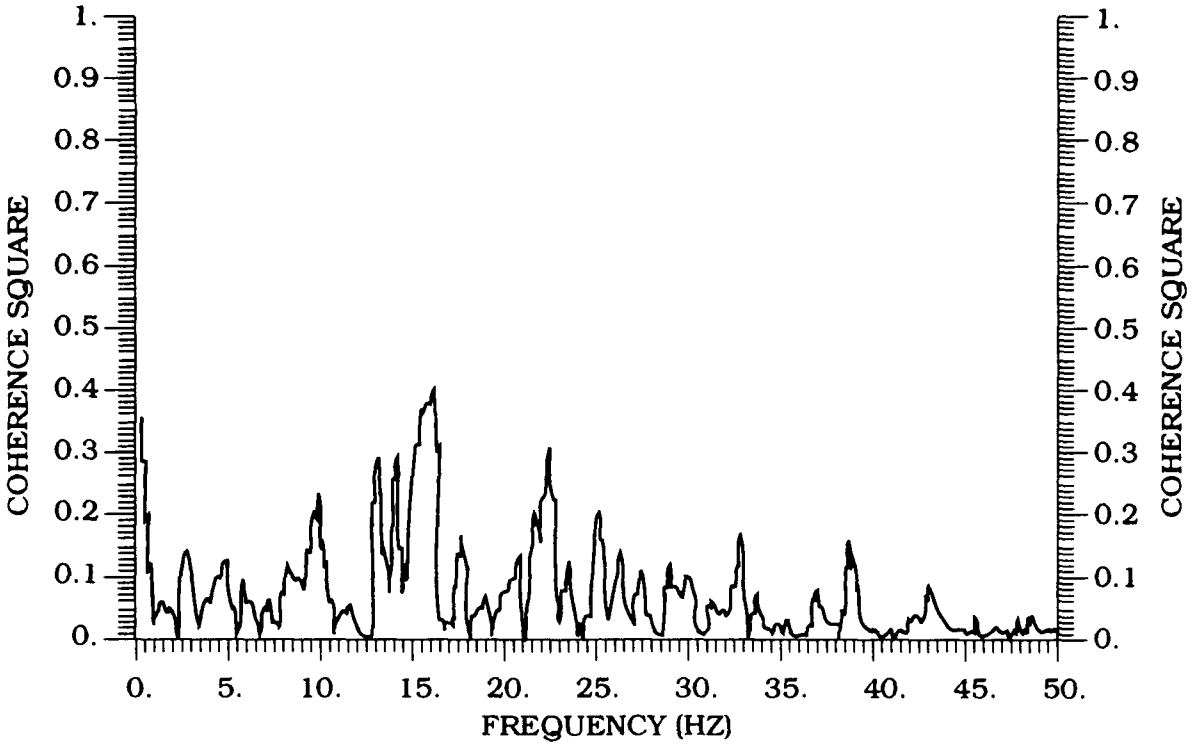

Figure 25. Coherency Squared Function Between Horizontal Seismic and Pressure Noise.

6.0 CONCLUSIONS

Analysis of seismic and atmospheric pressure noise environment data taken during the period 9 to 29 October 1986 at the La Junta, Colorado array site demonstrates that peak ambient conditions for this site and during this window, needed to define event detection capabilities, can adequately be modeled as Type II Gumbel extreme-value distributions. Further, it has been shown that there is at best only weak correlation between the various noise fields studied in both a broad and narrow-band sense.

References

1. Clark, T., and Stearn, C. (1960) *The Geological Evolution of North America*, The Ronald Press Co., New York.

2. von Glahn, P.G. (1980) *The Air Force Geophysics Laboratory Standalone Data Acquisition System: A Functional Description*, AFGL Report No. AFGL-TR-80-0317, ADA160253.

3. Bennett, W. (1948) Spectra of Quantized Signals, *Bell Systems Technical Journal*, **27** (No. 3):446-472.

4. Blackman, R., and Tukey, W. (1958) *The Measurement of Power Spectra*, Dover Publication, New York.

5. Aki, K., and Richards, P. (1980) *Quantitative Siesmology: Theory and Methods*, W. H. Freeman and Company, San Francisco.

6. Ringdal, F., and Bungum, H. (1977) Noise level variation at NORSAR and its effect on detectability, *Bull. Seism. Soc. Amer.*, 67 (No. 2):479-492.

7. Bruce, R. (1971) Field measurements: equipment and techniques, in *Noise and Vibration Control*, L. Beranek, ed., McGraw-Hill Book Company, New York.

8. Sax, R. (1968) Stationarity of seismic noise, *Geophysics*, **33** (No. 4):668-674.